Recursive graphical construction of Feynman diagrams and their multiplicities in ϕ^4 and $\phi^2 A$ theory

Hagen Kleinert,[1] Axel Pelster,[1] Boris Kastening,[2] and Michael Bachmann[1]

[1]*Institut für Theoretische Physik, Freie Universität Berlin, Arnimallee 14, 14195 Berlin, Germany*
[2]*Institut für Theoretische Physik, Universität Heidelberg, Philosophenweg 16, 69120 Heidelberg, Germany*

The free energy of a field theory can be considered as a functional of the free correlation function. As such it obeys a nonlinear functional differential equation that can be turned into a recursion relation. This is solved order by order in the coupling constant to find all connected vacuum diagrams with their proper multiplicities. The procedure is applied to a multicomponent scalar field theory with a ϕ^4 self-interaction and then to a theory of two scalar fields ϕ and A with an interaction $\phi^2 A$. All Feynman diagrams with external lines are obtained from functional derivatives of the connected vacuum diagrams with respect to the free correlation function. Finally, the recursive graphical construction is automatized by computer algebra with the help of a unique matrix notation for the Feynman diagrams.

I. INTRODUCTION

If one wants to draw all Feynman diagrams of higher orders by hand, it becomes increasingly difficult to identify all topologically different connections between the vertices. To count the corresponding multiplicities is an even more tedious task. Fortunately, there exist now various convenient computer programs, for instance, FEYNARTS [1–3] or QGRAF [4,5], for constructing and counting Feynman diagrams in different field theories.

The purpose of this paper is to develop an alternative systematic approach to construct all Feynman diagrams of a field theory. It relies on considering a Feynman diagram as a functional of its graphical elements, i.e., its lines and vertices. Functional derivatives with respect to these elements are represented by graphical operations that remove lines or vertices of a Feynman diagram in all possible ways. With these operations, our approach proceeds in two steps. First the connected vacuum diagrams are constructed, together with their proper multiplicities, as solutions of a graphical recursion relation derived from a nonlinear functional differential equation. This relation was set up a long time ago [6,7], but so far it has only been solved to all orders in the coupling strength in the trivial case of zero-dimensional quantum field theories. The present paper extends the previous work by developing an efficient graphical algorithm for solving this equation for two simple scalar field theories, a multicomponent scalar field theory with ϕ^4 self-interaction, and a theory with two scalar fields ϕ and A with the interaction $\phi^2 A$. In a second step, all connected diagrams with external lines are obtained from functional derivatives of the connected vacuum diagrams with respect to the free correlation function. Finally, we demonstrate how to automatize our construction method by computer algebra with the help of a unique matrix notation for Feynman diagrams.

II. SCALAR ϕ^4 THEORY

Consider a self-interacting scalar field ϕ with N components in d Euclidean dimensions whose thermal fluctuations are controlled by the energy functional

$$E[\phi] = \frac{1}{2} \int_{12} G_{12}^{-1} \phi_1 \phi_2 + \frac{g}{4!} \int_{1234} V_{1234} \phi_1 \phi_2 \phi_3 \phi_4 \tag{2.1}$$

with some coupling constant g. In this short-hand notation, the spatial and tensorial arguments of the field ϕ, the bilocal kernel G^{-1}, and the quartic interaction V are indicated by simple number indices, i.e.,

$$1 \equiv \{x_1, \alpha_1\}, \quad \int_1 \equiv \sum_{\alpha_1} \int d^d x_1,$$

$$\phi_1 \equiv \phi_{\alpha_1}(x_1), \quad G_{12}^{-1} \equiv G_{\alpha_1, \alpha_2}^{-1}(x_1, x_2),$$

$$V_{1234} \equiv V_{\alpha_1, \alpha_2, \alpha_3, \alpha_4}(x_1, x_2, x_3, x_4). \tag{2.2}$$

The kernel is a functional matrix G^{-1}, while V is a functional tensor, both being symmetric in their indices. The energy functional (2.1) describes generically d-dimensional Euclidean ϕ^4 theories. These are models for a family of universality classes of continuous phase transitions, such as the O(N)-symmetric ϕ^4 theory, which serves to derive the critical phenomena in dilute polymer solutions ($N=0$), Ising- and Heisenberg-like magnets ($N=1,3$), and superfluids ($N=2$). In all these cases, the energy functional (2.1) is specified by

$$G_{\alpha_1, \alpha_2}^{-1}(x_1, x_2) = \delta_{\alpha_1, \alpha_2}(-\partial_{x_1}^2 + m^2) \delta(x_1 - x_2), \tag{2.3}$$

$$V_{\alpha_1, \alpha_2, \alpha_3, \alpha_4}(x_1, x_2, x_3, x_4)$$

$$= \frac{1}{3} \{ \delta_{\alpha_1, \alpha_2} \delta_{\alpha_3, \alpha_4} + \delta_{\alpha_1, \alpha_3} \delta_{\alpha_2, \alpha_4} + \delta_{\alpha_1, \alpha_4} \delta_{\alpha_2, \alpha_3} \}$$

$$\times \delta(x_1 - x_2) \delta(x_1 - x_3) \delta(x_1 - x_4), \tag{2.4}$$

where the mass m^2 is proportional to the temperature distance from the critical point. In the following we shall leave G^{-1} and V completely general, except for the symmetry with respect to their indices, and insert the physical values

(2.3) and (2.4) at the end. By using natural units in which the Boltzmann constant k_B times the temperature T equals unity, the partition function is determined as a functional integral over the Boltzmann weight $e^{-E[\phi]}$

$$Z = \int \mathcal{D}\phi \, e^{-E[\phi]} \qquad (2.5)$$

and may be evaluated perturbatively as a power series in the coupling constant g. From this we obtain the negative free energy $W = \ln Z$ as an expansion

$$W = \sum_{p=0}^{\infty} \frac{1}{p!} \left(\frac{-g}{4!} \right)^p W^{(p)}. \qquad (2.6)$$

The coefficients $W^{(p)}$ may be displayed as connected vacuum diagrams constructed from lines and vertices. Each line represents a free correlation function

$$1 \;\underline{\qquad}\; 2 \;\equiv\; G_{12}, \qquad (2.7)$$

which is the functional inverse of the kernel G^{-1} in the energy functional (2.1), defined by

$$\int_2 G_{12} G_{23}^{-1} = \delta_{13}. \qquad (2.8)$$

The vertices represent an integral over the interaction

$$\times \quad \equiv \int_{1234} V_{1234}. \qquad (2.9)$$

To construct all connected vacuum diagrams contributing to $W^{(p)}$ to each order p in perturbation theory, one connects p vertices with $4p$ legs in all possible ways according to Feynman's rules, which follow from Wick's expansion of correlation functions into a sum of all pair contractions. This yields an increasing number of Feynman diagrams, each with a certain multiplicity that follows from combinatorics. In total there are $4!^p p!$ ways of ordering the $4p$ legs of the p vertices. This number is reduced by permutations of the legs and the vertices that leave a vacuum diagram invariant. Denoting the number of self-, double, triple, and fourfold connections with S, D, T, F, there are $2!^S$, $2!^D$, $3!^T$, $4!^F$ leg permutations. An additional reduction arises from the number N of vertex permutations, leaving the vacuum diagrams unchanged, where the vertices remain attached to the lines emerging from them in the same way as before. The resulting multiplicity of a connected vacuum diagram in the ϕ^4 theory is therefore given by the formula [9,10]

$$M_{\phi^4}^{E=0} = \frac{4!^p p!}{2!^{S+D} 3!^T 4!^F N}. \qquad (2.10)$$

The superscript $E = 0$ records that the number of external legs of the connected vacuum diagram is zero. The diagrammatic representation of the coefficients $W^{(p)}$ in the expansion (2.6) of the negative free energy W is displayed in Table I up to five loops [12–14].

For higher orders, the factorially increasing number of diagrams makes it more and more difficult to construct all topologically different diagrams and to count their multi-

plicities. In particular, it becomes quite hard to identify by inspection the number N of vertex permutations. This identification problem is solved by introducing a uniqued matrix notation for the diagrams, to be explained in detail in Sec. IV.

In the following, we shall generate iteratively all connected vacuum diagrams. We start in Sec. II A by identifying graphical operations associated with functional derivatives with respect to the kernel G^{-1}, or the free correlation function G. In Sec. II B we show that these operations can be applied to the one-loop contribution of the free partition function to generate all perturbative contributions to the partition function (2.5). In Sec. II C we derive a nonlinear functional differential equation for the negative free energy W, whose graphical solution in Sec. II D yields all connected vacuum diagrams order by order in the coupling strength.

A. Basic graphical operations

Each Feynman diagram is composed of integrals over products of free correlation functions G and may thus be considered as a functional of the kernel G^{-1}. The connected vacuum diagrams satisfy a certain functional differential equation, from which they will be constructed recursively. This will be done by a graphical procedure, for which we set up the necessary graphical rules in this subsection. First we observe that functional derivatives with respect to the kernel G^{-1} or to the free correlation function G correspond to the graphical prescriptions of cutting or of removing a single line of a diagram in all possible ways, respectively.

1. Cutting lines

Since ϕ is a real scalar field, the kernel G^{-1} is a symmetric functional matrix. This property has to be taken into account when performing functional derivatives with respect to the kernel G^{-1}, whose basic rule is

$$\frac{\delta G_{12}^{-1}}{\delta G_{34}^{-1}} = \frac{1}{2} \{ \delta_{13}\delta_{42} + \delta_{14}\delta_{32} \}. \qquad (2.11)$$

From the identity (2.8) and the functional chain rule, we find the effect of this derivative on the free correlation function
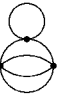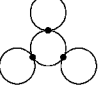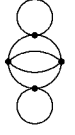
$$-2 \frac{\delta G_{12}}{\delta G_{34}^{-1}} = G_{13}G_{42} + G_{14}G_{32}. \qquad (2.12)$$

This has the graphical representation

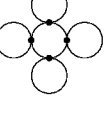$$-2 \frac{\delta}{\delta G_{34}^{-1}} 1 \underline{\quad} 2 = 1 \underline{\quad} 3 \;\; 4 \underline{\quad} 2 + 1 \underline{\quad} 4 \;\; 3 \underline{\quad} 2. \qquad (2.13)$$

Thus differentiating a free correlation function with respect to the kernel G^{-1} amounts to cutting the associated line into two pieces. The differentiation rule (2.11) ensures that the spatial indices of the kernel are symmetrically attached to the newly created line ends in the two possible ways. When differentiating a general Feynman integral with respect to G^{-1}, the product rule of functional differentiation leads to a sum of diagrams in which each line is cut once.

TABLE I. Connected vacuum diagrams and their multiplicities of the ϕ^4 theory up to five loops. Each diagram is characterized by the vector $(S,D,T,F;N)$ whose components specify the number of self-, double, triple, and fourfold connections, and of the vertex permutations leaving the vacuum diagram unchanged, respectively.

p	$W^{(p)}$
1	#1 3 (2,1,0,0;1)
2	#2 24 (0,0,0,1;2) #3 72 (2,1,0,0;2)
3	#4 1728 (0,3,0,0;6) #5 3456 (1,0,1,0;2) #6 1728 (3,0,0,0;6) #7 2592 (2,2,0,0;2)
4	#8 62208 (0,4,0,0;8) #9 248832 (0,2,0,0;8) #10 55296 (0,0,2,0;4) #11 497664 (1,2,0,0;2) #12 165888 (2,0,1,0;2) #13 248832 (2,1,0,0;4) #14 165888 (1,1,1,0;2) #15 248832 (3,1,0,0;2) #16 62208 (4,0,0,0;8) #17 124416 (2,3,0,0;2)

With this graphical operation, the product of two fields can be rewritten as a derivative of the energy functional with respect to the kernel

$$\phi_1 \phi_2 = 2 \frac{\delta E[\phi]}{\delta G_{12}^{-1}}, \qquad (2.14)$$

as follows directly from (2.1) and (2.11). Applying the substitution rule (2.14) to the functional integral for the fully interacting two-point function

$$\mathbf{G}_{12} = \frac{1}{Z} \int \mathcal{D}\phi \; \phi_1 \phi_2 e^{-E[\phi]}, \qquad (2.15)$$

we obtain the fundamental identity

$$\mathbf{G}_{12} = -2 \frac{\delta W}{\delta G_{12}^{-1}}. \qquad (2.16)$$

Thus, by cutting a line of the connected vacuum diagrams in all possible ways, we obtain all diagrams of the fully interacting two-point function. Analytically this has a Taylor series expansion in powers of the coupling constant g similar to (2.6)

$$\mathbf{G}_{12} = \sum_{p=0}^{\infty} \frac{1}{p!} \left(\frac{-g}{4!} \right)^p \mathbf{G}_{12}^{(p)} \qquad (2.17)$$

with coefficients

$$\mathbf{G}_{12}^{(p)} = -2 \frac{\delta W^{(p)}}{\delta G_{12}^{-1}}. \qquad (2.18)$$
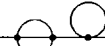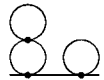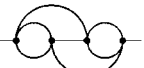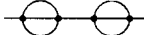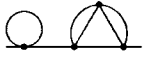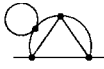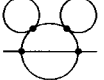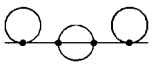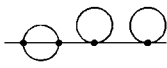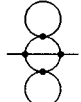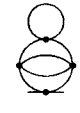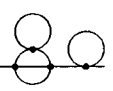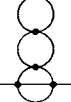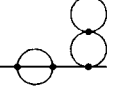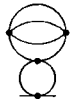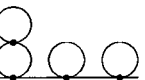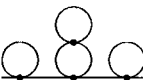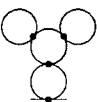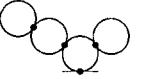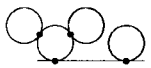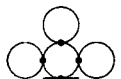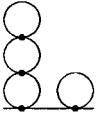
The cutting prescription (2.18) converts the vacuum diagrams of pth order in the coefficients $W^{(p)}$ in Table I to the corresponding ones in the coefficients $\mathbf{G}_{12}^{(p)}$ of the two-point function. The results are shown in Table II up to four loops. The numbering of diagrams used in Table II reveals from which connected vacuum diagrams they are obtained by cutting a line. For instance, the diagrams 15.1–15.5 and their multiplicities in Table II follow from the connected vacuum diagram 15 in Table I. We observe that the multiplicity of a diagram of a two-point function obeys a formula similar to (2.10):

$$M_{\phi^4}^{E=2} = \frac{4!^p p! 2!}{2!^{S+D} 3!^T N}. \qquad (2.19)$$

In the numerator, the $4!^p p!$ permutations of the $4p$ legs of the p vertices are multiplied by a factor 2! for the permutations of the $E=2$ end points of the two-point function. The number N in the denominator counts the combined permutations of the p vertices and the two end points that leave the diagram unchanged.

Performing a differentiation of the two-point function (2.15) with respect to the kernel G^{-1} yields

TABLE II. Connected diagrams of the two-point function and their multiplicities of the ϕ^4 theory up to four loops. Each diagram is characterized by the vector $(S,D,T;N)$ whose components specify the number of self-, double, triple connections, and of the combined permutations of vertices and external lines leaving the diagram unchanged, respectively.

p	$G_{12}^{(p)}$
1	#1.1 12 $(1,0,0;2)$
2	#2.1 192 $(0,0,1;2)$ #3.1 288 $(1,1,0;2)$ #3.2 288 $(2,0,0;2)$
3	#4.1 20736 $(0,2,0;2)$ #5.1 6912 $(0,0,1;4)$ #5.2 20736 $(1,1,0;2)$ #5.3 13824 $(1,0,1;1)$ #6.1 10368 $(2,0,0;4)$ #6.2 10368 $(3,0,0;2)$ #7.1 10368 $(1,2,0;2)$ #7.2 20736 $(2,1,0;1)$
4	#8.1 995328 $(0,3,0;2)$ #9.1 1990656 $(0,1,0;4)$ #9.2 1990656 $(0,2,0;2)$ #10.1 221184 $(0,0,2;2)$ #10.2 663552 $(0,1,1;2)$ #11.1 995328 $(0,2,0;4)$ #11.2 1990656 $(1,2,0;1)$ #11.3 995328 $(1,2,0;2)$ #11.4 3981312 $(1,1,0;1)$ #12.1 995328 $(2,1,0;2)$ #12.2 331776 $(2,0,1;2)$ #12.3 663552 $(2,0,1;1)$ #12.4 663552 $(1,0,1;2)$ #13.1 995328 $(2,0,0;4)$ #13.2 995328 $(1,1,0;4)$ #13.3 1990656 $(2,1,0;1)$ #14.1 995328 $(1,2,0;2)$ #14.2 663552 $(1,1,1;1)$ #14.3 663552 $(1,0,1;2)$ #14.4 331776 $(0,1,1;4)$ #15.1 995328 $(3,1,0;1)$ #15.2 497664 $(3,1,0;2)$ #15.3 497664 $(2,1,0;4)$ #15.4 995328 $(2,1,0;2)$ #15.5 995328 $(3,0,0;2)$ #16.1 497664 $(3,0,0;4)$ #16.2 497664 $(4,0,0;2)$ #17.1 497664 $(1,3,0;2)$ #17.2 995328 $(2,2,0;1)$ #17.3 497664 $(2,2,0;2)$

$$-2\frac{\delta \mathbf{G}_{12}}{\delta G_{34}^{-1}}=\mathbf{G}_{1234}-\mathbf{G}_{12}\mathbf{G}_{34}, \tag{2.20}$$

where $\mathbf{G}_{1234}$ denotes the fully interacting four-point function

$$\mathbf{G}_{1234}=\frac{1}{Z}\int \mathcal{D}\phi \ \phi_1\phi_2\phi_3\phi_4 e^{-E[\phi]}. \tag{2.21}$$

The term $\mathbf{G}_{12}\mathbf{G}_{34}$ in (2.20) subtracts a certain set of disconnected diagrams from $\mathbf{G}_{1234}$. By subtracting all disconnected diagrams from $\mathbf{G}_{1234}$, we obtain the connected four-point function

$$\mathbf{G}_{1234}^{c}\equiv\mathbf{G}_{1234}-\mathbf{G}_{12}\mathbf{G}_{34}-\mathbf{G}_{13}\mathbf{G}_{24}-\mathbf{G}_{14}\mathbf{G}_{23} \tag{2.22}$$

in the form

$$\mathbf{G}_{1234}^{c}=-2\frac{\delta \mathbf{G}_{12}}{\delta G_{34}^{-1}}-\mathbf{G}_{13}\mathbf{G}_{24}-\mathbf{G}_{14}\mathbf{G}_{23}. \tag{2.23}$$

The first term contains all diagrams obtained by cutting a line in the diagrams of the two-point function $\mathbf{G}_{12}$. The second and third terms remove from these the disconnected diagrams. In this way we obtain the perturbative expansion

$$\mathbf{G}_{1234}^{c}=\sum_{p=1}^{\infty}\frac{1}{p!}\left(\frac{-g}{4!}\right)^{p}\mathbf{G}_{1234}^{c,(p)} \tag{2.24}$$

with coefficients

$$\mathbf{G}_{1234}^{c,(p)}=-2\frac{\delta \mathbf{G}_{12}^{(p)}}{\delta G_{34}^{-1}}-\sum_{q=0}^{p}\binom{p}{q}(\mathbf{G}_{13}^{(p-q)}\mathbf{G}_{24}^{(q)}+\mathbf{G}_{14}^{(p-q)}\mathbf{G}_{23}^{(q)}). \tag{2.25}$$

They are listed diagrammatically in Table III up to three loops. As before in Table II, the multiple numbering in Table III indicates the origin of each diagram of the connected four-point function. For instance, the diagram 11.2.2, 11.4.3, 14.1.2, 14.3.3 in Table III stems together with its multiplicity from the diagrams 11.2, 11.4, 14.1, 14.3 in Table II.

The multiplicity of each diagram of a connected four-point function obeys a formula similar to (2.19):

$$M_{\phi^4}^{E=4}=\frac{4!^p p!4!}{2!^{S+D}3!^T N}. \tag{2.26}$$

This multiplicity decomposes into equal parts if the spatial indices 1, 2, 3, 4 are assigned to the $E=4$ end points of the connected four-point function, for instance:

$$\tag{2.27}$$

Generalizing the multiplicities (2.10), (2.19), and (2.26) for connected vacuum diagrams, two- and four-point functions to an arbitrary connected correlation function with an even number E of end points, we see that

$$M_{\phi^4}^{E}=\frac{4!^p p!E!}{2!^{S+D}3!^T 4!^F N}, \tag{2.28}$$

where N counts the number of combined permutations of vertices and external lines which leave the diagram unchanged.

2. Removing lines

We now study the graphical effect of functional derivatives with respect to the free correlation function G, where the basic differentiation rule (2.11) becomes

$$\frac{\delta G_{12}}{\delta G_{34}}=\frac{1}{2}\{\delta_{13}\delta_{42}+\delta_{14}\delta_{32}\}. \tag{2.29}$$

We represent this graphically by extending the elements of Feynman diagrams by an open dot with two labeled line ends representing the delta function:

$$1\!-\!\circ\!-\!2=\delta_{12} \tag{2.30}$$

Thus we can write the differentiation (2.29) graphically as follows:

$$\frac{\delta}{\delta 3\!-\!4}\,1\!-\!-\!2=\frac{1}{2}\left\{1\!-\!\circ\!-3\ 4\!-\!\circ\!-2+1\!-\!\circ\!-4\ 3\!-\!\circ\!-2\right\}. \tag{2.31}$$

Differentiating a line with respect to the free correlation function removes the line, leaving in a symmetrized way the spatial indices of the free correlation function on the vertices to which the line was connected.

The effect of this derivative is illustrated by studying the diagrammatic effect of the operator

$$\hat{L}=\int_{12}G_{12}\frac{\delta}{\delta G_{12}}. \tag{2.32}$$

Applying $\hat{L}$ to a connected vacuum diagram in $W^{(p)}$, the functional derivative $\delta/\delta G_{12}$ generates diagrams in each of which one of the $2p$ lines of the original vacuum diagram is removed. Subsequently, the removed lines are again reinserted, so that the connected vacuum diagrams $W^{(p)}$ are eigenfunctions of $\hat{L}$, whose eigenvalues $2p$ count the lines of the diagrams:

$$\hat{L}W^{(p)}=2pW^{(p)}. \tag{2.33}$$

TABLE III. Connected diagrams of the four-point function and their multiplicities of the ϕ^4 theory up to three loops. Each diagram is characterized by the vector $(S, D, T; N)$ whose components specify the number of self-, double, triple connections, and of the combined permutations of vertices and external lines leaving the diagram unchanged, respectively.
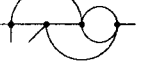
p	$G^{c,(p)}_{1234}$		
1	#1.1.1 24 $(0,0,0;24)$		
2	#2.1.1,#3.1.1 1152,576 1728 $(0,1,0;8)$	#3.1.2,#3.2.1 1152,1152 2304 $(1,0,0;6)$	
3	#4.1.1,#7.1.1 41472,20736 62208 $(0,2,0;8)$	#4.1.2,#5.1.1,#5.2.1 165888,41472,41472 248832 $(0,1,0;4)$	#5.1.2,#5.3.2 27648,27648 55296 $(0,0,1;6)$
	#5.2.2,#6.1.1 82944,41472 124416 $(1,0,0;8)$	#5.2.3,#5.3.1,#7.1.2,#7.2.1 82944,82944,41472,41472 248832 $(1,1,0;2)$	#6.1.2,#6.2.2,#7.2.2 20736,20736,82944 124416 $(2,0,0;4)$
	#6.1.3,#6.2.1 41472,41472 82944 $(2,0,0;6)$	#7.1.3,#7.2.3 41472,41472 82944 $(1,1,0;6)$	
4	#8.1.1,#17.1.1 1990656,995328 2985984 $(0,3,0;8)$	#8.1.2,#9.2.1,#10.2.1 3981312,3981312,3981312 11943936 $(0,2,0;4)$	#8.1.3,#11.1.2,#11.3.1 7962624,1990656,1990656 11943936 $(0,2,0;4)$
	#9.1.1,#13.2.1 3981312,1990656 5971968 $(0,1,0;16)$	#9.1.2 7962624 $(0,0,0;24)$	#9.1.3,#9.2.3,#11.1.1,#11.4.1 15925248,15925248,7962624,7962624 47775744 $(0,1,0;2)$
	#9.2.2,#14.1.1,#14.4.3 7962624,1990656,1990656 11943936 $(0,2,0;4)$	#10.1.1,#10.2.3,#14.2.1,#14.4.2 2654208,2654208,1327104,1327104 7962624 $(0,1,1;2)$	#10.2.2,#12.4.1 2654208,1327104 3981312 $(0,0,1;8)$
	#11.1.3,#11.2.1 3981312,3981312 7962624 $(0,2,0;6)$	#11.2.2,#11.4.3,#14.1.2,#14.3.3 7962624,7962624,3981312,3981312 23887872 $(1,1,0;2)$	#11.2.3,#11.4.2,#13.2.2,#13.3.1 7962624,7962624,3981312,3981312 23887872 $(1,1,0;2)$
	#11.2.4,#11.3.2,#17.1.2,#17.2.1 3981312,3981312,1990656,1990656 11943936 $(1,2,0;2)$	#11.3.3,#11.4.4,#12.1.1,#12.4.5 7962624,7962624,3981312,3981312 23887872 $(1,1,0;2)$	#11.4.5,#15.3.1,#15.4.1 7962624,1990656,1990656 11943936 $(1,1,0;4)$

TABLE III. (Continued).

#11.4.6,#13.1.1,#13.2.3

15925248,3981312,3981312

23887872

(1,0,0;4)

#12.1.2,#12.2.2,#13.3.3,#17.2.2

1990656,1990656,3981312,3981312

11943936

(2,1,0;2)

#12.1.3,#16.1.2

3981312,1990656

5971968

(2,0,0;8)

#12.1.4,#12.3.3,#15.1.1,#15.3.2

3981312,3981312,1990656,1990656

11943936

(2,1,0;2)

#12.2.1,#12.4.2

1327104,1327104

2654208

(1,0,1;6)

#12.3.2,#12.4.3,#14.2.2,#14.3.2

1327104,1327104,2654208,2654208

7962624

(1,0,1;2)

#12.3.1,#12.4.4

1327104,1327104

2654208

(1,0,1;6)

#13.1.2,#13.3.4,#15.4.2,#15.5.1

7962624,7962624,3981312,3981312

23887872

(2,0,0;2)

#13.1.3,#16.1.1

1990656,995328

2985984

(2,0,0;16)

#13.2.4,#13.3.5

3981312,3981312

7962624

(1,1,0;6)

#13.3.2,#15.2.1,#15.3.3

3981312,995328,995328

5971968

(2,1,0;4)

#14.1.3,#14.2.3,#17.1.3,#17.3.1

3981312,3981312,1990656,1990656

11943936

(1,2,0;2)

#14.1.4,#15.4.4

3981312,1990656

5971968

(1,1,0;8)

#14.3.1,#14.4.1

1327104,1327104

2654208

(0,0,1;12)

#15.1.2,#15.5.3,#16.1.3,#16.2.2

3981312,3981312,1990656,1990656

11943936

(3,0,0;2)

#15.1.3,#15.4.3,#17.2.3,#17.3.2

1990656,1990656,3981312,3981312

11943936

(2,1,0;2)

#15.1.4,#15.4.5

1990656,1990656

3981312

(2,1,0;6)

#15.2.2,#15.5.2

1990656,1990656

3981312

(3,0,0;6)

#15.2.3,#15.4.6

1990656,1990656

3981312

(2,1,0;6)

#15.3.4,#15.5.4

1990656,1990656

3981312

(2,0,0;12)

#16.1.4,#16.2.1

1990656,1990656

3981312

(3,0,0;6)

#17.1.4,#17.2.4

1990656,1990656

3981312

(1,2,0;6)

As an example, take the explicit first-order expression for the vacuum diagrams, i.e.

$$W^{(1)} = 3 \int_{1234} V_{1234} G_{12} G_{34}, \qquad (2.34)$$

and apply the basic rule (2.29), leading to the desired eigenvalue 2.

B. Perturbation theory

Field theoretic perturbation expressions are usually derived by introducing an external current J into the energy functional (2.1) which is linearly coupled to the field ϕ [15–17]. Thus the partition function (2.5) becomes in the presence of J the generating functional $Z[J]$, which allows us to

find all free n-point functions from functional derivatives with respect to this external current J. In the normal phase of a ϕ^4 theory, the expectation value of the field ϕ is zero and only correlation functions of an even number of fields are nonzero. To calculate all of these, it is possible to substitute two functional derivatives with respect to the current J by one functional derivative with respect to the kernel G^{-1}. This reduces the number of functional derivatives in each order of perturbation theory by one-half and has the additional advantage that the introduction of the current J becomes superfluous.

1. Current approach

Recall briefly the standard perturbative treatment, in which the energy functional (2.1) is artificially extended by a source term

$$E[\phi,J]=E[\phi]-\int_1 J_1\phi_1. \qquad (2.35)$$

The functional integral for the generating functional

$$Z[J]=\int \mathcal{D}\phi \, e^{-E[\phi,J]} \qquad (2.36)$$

is first explicitly calculated for a vanishing coupling constant g, yielding

$$Z^{(0)}[J]=\exp\left\{ -\frac{1}{2}\operatorname{Tr}\ln G^{-1}+\frac{1}{2}\int_{12} G_{12}J_1J_2\right\}, \qquad (2.37)$$

where the trace of the logarithm of the kernel is defined by the series (see p. 16 in Ref. [18])

$$\operatorname{Tr}\ln G^{-1}=\sum_{n=1}^{\infty} \frac{(-1)^{n+1}}{n}\int_{1\ldots n}\{G_{12}^{-1}-\delta_{12}\}\cdots\{G_{n1}^{-1}-\delta_{n1}\}. \qquad (2.38)$$

If the coupling constant g does not vanish, one expands the generating functional $Z[J]$ in powers of the quartic interaction V, and reexpresses the resulting powers of the field within the functional integral (2.36) as functional derivatives with respect to the current J. The original partition function (2.5) can thus be obtained from the free generating functional (2.37) by the formula

$$Z=\exp\left\{-\frac{g}{4!}\int_{1234}V_{1234}\frac{\delta^4}{\delta J_1\delta J_2\delta J_3\delta J_4}\right\}Z^{(0)}[J]\Bigg|_{J=0}. \qquad (2.39)$$

Expanding the exponential in a power series, we arrive at the perturbation expansion

$$Z=\left\{1+\frac{-g}{4!}\int_{1234}V_{1234}\frac{\delta^4}{\delta J_1\delta J_2\delta J_3\delta J_4}\right.$$
$$+\frac{1}{2}\left(\frac{-g}{4!}\right)^2\int_{12345678}V_{1234}V_{5678}$$
$$\left.\times\frac{\delta^8}{\delta J_1\delta J_2\delta J_3\delta J_4\delta J_5\delta J_6\delta J_7\delta J_8}+\ldots\right\}Z^{(0)}[J]\Bigg|_{J=0}, \qquad (2.40)$$

in which the pth order contribution for the partition function requires the evaluation of $4p$ functional derivatives with respect to the current J.

2. Kernel approach

The derivation of the perturbation expansion simplifies, if we use functional derivatives with respect to the kernel G^{-1} in the energy functional (2.1) rather than with respect to the current J. This allows us to substitute the previous expression (2.39) for the partition function by

$$Z=\exp\left\{ -\frac{g}{6}\int_{1234}V_{1234}\frac{\delta^2}{\delta G_{12}^{-1}\delta G_{34}^{-1}}\right\}e^{W^{(0)}}, \qquad (2.41)$$

where the zeroth order of the negative free energy has the diagrammatic representation

$$W^{(0)}=-\frac{1}{2}\operatorname{Tr}\ln G^{-1}\equiv\frac{1}{2}\bigcirc . \qquad (2.42)$$

Expanding again the exponential in a power series, we obtain

$$Z=\left\{1+\frac{-g}{6}\int_{1234}V_{1234}\frac{\delta^2}{\delta G_{12}^{-1}\delta G_{34}^{-1}}\right.$$
$$+\frac{1}{2}\left(\frac{-g}{6}\right)^2\int_{12345678}V_{1234}V_{5678}$$
$$\left.\times\frac{\delta^4}{\delta G_{12}^{-1}\delta G_{34}^{-1}\delta G_{56}^{-1}\delta G_{78}^{-1}}+\ldots\right\}e^{W^{(0)}}. \qquad (2.43)$$

Thus we need only half as many functional derivatives than in (2.40). Taking into account (2.11), (2.12), and (2.38), we obtain

$$\frac{\delta W^{(0)}}{\delta G_{12}^{-1}}=-\frac{1}{2}G_{12}, \quad \frac{\delta^2 W^{(0)}}{\delta G_{12}^{-1}\delta G_{34}^{-1}}=\frac{1}{4}\{G_{13}G_{24}+G_{14}G_{23}\}, \qquad (2.44)$$

such that the partition function Z becomes

$$Z=\left\{1+\frac{-g}{4!}3\int_{1234}V_{1234}G_{12}G_{34}+\frac{1}{2}\left(\frac{-g}{4!}\right)^2\right.$$
$$\times\int_{12345678}V_{1234}V_{5678}\left[9G_{12}G_{34}G_{56}G_{78}\right.$$
$$\left.\left.+24G_{15}G_{26}G_{37}G_{48}+72G_{12}G_{35}G_{46}G_{78}\right]+\ldots\right\}e^{W^{(0)}}. \qquad (2.45)$$

This has the diagrammatic representation

$$Z = \left\{ 1 + \frac{-g}{4!} 3 \; \bigcirc\bigcirc + \frac{1}{2}\left(\frac{-g}{4!}\right)^2 \left[9 \; \bigcirc\bigcirc \; \bigcirc\bigcirc + 24 \; \ominus\!\!\!\!\ominus + 72 \; \bigcirc\bigcirc\bigcirc \right] + \dots \right\} e^{\frac{1}{2} \bigcirc} \tag{2.46}$$

All diagrams in this expansion follow directly by successively cutting lines of the basic one-loop vacuum diagram (2.42) according to (2.43). By going to the logarithm of the partition function Z, we find a diagrammatic expansion for the negative free energy W

$$W = \frac{1}{2} \; \bigcirc + \frac{-g}{4!} 3 \; \bigcirc\bigcirc + \frac{1}{2}\left(\frac{-g}{4!}\right)^2 \left\{ 24 \; \ominus\!\!\!\!\ominus + 72 \; \bigcirc\bigcirc\bigcirc \right\} + \dots , \tag{2.47}$$

which turns out to contain precisely all connected diagrams in (2.46) with the same multiplicities. In the next section we show that this diagrammatic expansion for the negative free energy can be derived more efficiently by solving a functional differential equation.

C. Functional differential equation for $W = \ln Z$

Regarding the partition function Z as a functional of the kernel G^{-1}, we derive a functional differential equation for Z. We start with the trivial identity

$$\int \mathcal{D}\phi \, \frac{\delta}{\delta \phi_1} \{\phi_2 e^{-E[\phi]}\} = 0, \tag{2.48}$$

which follows via direct functional integration from the vanishing of the exponential at infinite fields. Taking into account the explicit form of the energy functional (2.1), we perform the functional derivative with respect to the field and obtain

$$\int \mathcal{D}\phi \left\{ \delta_{12} - \int_3 G_{13}^{-1} \phi_2 \phi_3 \right.$$
$$\left. - \frac{g}{6} \int_{345} V_{1345} \phi_2 \phi_3 \phi_4 \phi_5 \right\} e^{-E[\phi]} = 0. \tag{2.49}$$

Applying the substitution rule (2.14), this equation can be expressed in terms of the partition function (2.5) and its derivatives with respect to the kernel G^{-1}:

$$\delta_{12} Z + 2 \int_3 G_{13}^{-1} \frac{\delta Z}{\delta G_{23}^{-1}} = \frac{2}{3} g \int_{345} V_{1345} \frac{\delta^2 Z}{\delta G_{23}^{-1} \delta G_{45}^{-1}}. \tag{2.50}$$

Note that this linear functional differential equation for the partition function Z is, indeed, solved by (2.41) due to the commutation relation

$$\exp\left\{ -\frac{g}{6} \int_{1234} V_{1234} \frac{\delta^2}{\delta G_{12}^{-1} \delta G_{34}^{-1}} \right\} G_{56}^{-1} - G_{56}^{-1}$$
$$\times \exp\left\{ -\frac{g}{6} \int_{1234} V_{1234} \frac{\delta^2}{\delta G_{12}^{-1} \delta G_{34}^{-1}} \right\}$$
$$= -\frac{g}{3} \int_{78} V_{5678} \frac{\delta}{\delta G_{78}^{-1}}$$
$$\times \exp\left\{ -\frac{g}{6} \int_{1234} V_{1234} \frac{\delta^2}{\delta G_{12}^{-1} \delta G_{34}^{-1}} \right\}, \tag{2.51}$$

which follows from the canonical one

$$\frac{\delta}{\delta G_{12}^{-1}} G_{34}^{-1} - G_{34}^{-1} \frac{\delta}{\delta G_{12}^{-1}} = \frac{1}{2} \{ \delta_{13} \delta_{24} + \delta_{14} \delta_{23} \}. \tag{2.52}$$

Going over from Z to $W = \ln Z$, the linear functional differential equation (2.50) turns into a nonlinear one:

$$\delta_{12} + 2 \int_3 G_{13}^{-1} \frac{\delta W}{\delta G_{23}^{-1}}$$
$$= \frac{2}{3} g \int_{345} V_{1345} \left\{ \frac{\delta^2 W}{\delta G_{23}^{-1} \delta G_{45}^{-1}} + \frac{\delta W}{\delta G_{23}^{-1}} \frac{\delta W}{\delta G_{45}^{-1}} \right\}. \tag{2.53}$$

If the coupling constant g vanishes, this is immediately solved by (2.42). For a non-vanishing coupling constant g, the right-hand side in (2.53) produces corrections to (2.42) which we shall denote with $W^{(\mathrm{int})}$. Thus the negative free energy W decomposes according to

$$W = W^{(0)} + W^{(\mathrm{int})}. \tag{2.54}$$

Inserting this into (2.53) and taking into account (2.44), we obtain the following functional differential equation for the interaction negative free energy $W^{(\mathrm{int})}$:

$$\int_{12} G_{12}^{-1} \frac{\delta W^{(\mathrm{int})}}{\delta G_{12}^{-1}}$$

$$= \frac{g}{4} \int_{1234} V_{1234} G_{12} G_{34} - \frac{g}{3} \int_{1234} V_{1234} G_{12} \frac{\delta W^{(\mathrm{int})}}{\delta G_{34}^{-1}}$$

$$+ \frac{g}{3} \int_{1234} V_{1234} \left\{ \frac{\delta^2 W^{(\mathrm{int})}}{\delta G_{12}^{-1} \delta G_{34}^{-1}} + \frac{\delta W^{(\mathrm{int})}}{\delta G_{12}^{-1}} \frac{\delta W^{(\mathrm{int})}}{\delta G_{34}^{-1}} \right\}.$$

$$(2.55)$$

With the help of the functional chain rule, the first and second derivatives with respect to the kernel G^{-1} are rewritten as

$$\frac{\delta}{\delta G_{12}^{-1}} = - \int_{34} G_{13} G_{24} \frac{\delta}{\delta G_{34}} \qquad (2.56)$$

and

$$\frac{\delta^2}{\delta G_{12}^{-1} \delta G_{34}^{-1}} = \int_{5678} G_{15} G_{26} G_{37} G_{48} \frac{\delta^2}{\delta G_{56} \delta G_{78}}$$

$$+ \frac{1}{2} \int_{56} \{ G_{13} G_{25} G_{46} + G_{14} G_{25} G_{36}$$

$$+ G_{23} G_{15} G_{46} + G_{24} G_{15} G_{36} \} \frac{\delta}{\delta G_{56}},$$

$$(2.57)$$

respectively, so that the functional differential equation (2.55) for $W^{(\mathrm{int})}$ takes the form (compare Eq. (51) in Ref. [7])

$$\int_{12} G_{12} \frac{\delta W^{(\mathrm{int})}}{\delta G_{12}} = - \frac{g}{4} \int_{1234} V_{1234} G_{12} G_{34}$$

$$- g \int_{123456} V_{1234} G_{12} G_{35} G_{46} \frac{\delta W^{(\mathrm{int})}}{\delta G_{56}}$$

$$- \frac{g}{3} \int_{12345678} V_{1234} G_{15} G_{26} G_{37} G_{48}$$

$$\times \left\{ \frac{\delta^2 W^{(\mathrm{int})}}{\delta G_{56} \delta G_{78}} + \frac{\delta W^{(\mathrm{int})}}{\delta G_{56}} \frac{\delta W^{(\mathrm{int})}}{\delta G_{78}} \right\}.$$

$$(2.58)$$

D. Recursion relation and graphical solution

We now convert the functional differential equation (2.58) into a recursion relation by expanding $W^{(\mathrm{int})}$ into a power series in g:

$$W^{(\mathrm{int})} = \sum_{p=1}^{\infty} \frac{1}{p!} \left(\frac{-g}{4!} \right)^p W^{(p)}. \qquad (2.59)$$

Using the property (2.33) that the coefficient $W^{(p)}$ satisfies the eigenvalue problem of the line numbering operator (2.32), we obtain the recursion relation

$$W^{(p+1)} = 12 \int_{123456} V_{1234} G_{12} G_{35} G_{46} \frac{\delta W^{(p)}}{\delta G_{56}}$$

$$+ 4 \int_{12345678} V_{1234} G_{15} G_{26} G_{37} G_{48} \frac{\delta^2 W^{(p)}}{\delta G_{56} \delta G_{78}}$$

$$+ 4 \sum_{q=1}^{p-1} \binom{p}{q} \int_{12345678} V_{1234} G_{15} G_{26} G_{37} G_{48}$$

$$\times \frac{\delta W^{(p-q)}}{\delta G_{56}} \frac{\delta W^{(q)}}{\delta G_{78}} \qquad (2.60)$$

and the initial condition (2.34). With the help of the graphical rules of Sec. II A, the recursion relation (2.60) can be written diagrammatically as follows:

$$(2.61)$$

This is iterated starting from

$$(2.62)$$

The right-hand side of (2.61) contains three different graphical operations. The first two are linear and involve one- or two-line amputations of the previous perturbative order. The third operation is nonlinear and mixes two different one-line amputations of lower orders.

An alternative way of formulating the above recursion relation may be based on the graphical rules

$$W^{(p)} = \left(p\right) , \qquad \frac{\delta W^{(p)}}{\delta G_{12}} = {}_2^1\left(p\right) , \qquad \frac{\delta^2 W^{(p)}}{\delta G_{12}\delta G_{34}} = {}_3^2{}^1\left(p\right)_4 . \tag{2.63}$$

With these, the recursion relation (2.61) reads

$$\left(p+1\right) = 4\left(p\right) + 12\,\bigcirc\!\!\!<\!\left(p\right) + 4\sum_{q=1}^{p-1}\binom{p}{q}\bigcirc\!\!\!<\!(p-q)\!\!\bowtie\!(q)\!\!>\!\bigcirc , \qquad p \geq 1. \tag{2.64}$$

To demonstrate the working of (2.61), we calculate the connected vacuum diagrams up to five loops. Applying the linear operations to (2.60), we obtain immediately

$$\frac{\delta W^{(1)}}{\delta 1\!-\!2} = 6\; {}_2^1\!\!>\!\!\bigcirc , \qquad \frac{\delta^2 W^{(1)}}{\delta 1\!-\!2\,\delta 3\!-\!4} = 6\; {}_2^1\!\!>\!\!<\!{}_4^3 . \tag{2.65}$$

Inserted into (2.61), these lead to the three-loop vacuum diagrams

$$W^{(2)} = 24\;\ominus + 72\;\bigcirc\!\bigcirc\!\bigcirc . \tag{2.66}$$

Proceeding to the next order, we have to perform one- and two-line amputations on the vacuum diagrams in (2.66), leading to

$$\frac{\delta W^{(2)}}{\delta 1\!-\!2} = 96\; {}_1\!-\!\ominus\!-\!{}_2 + 144\; {}_1\!\overset{\bigcirc}{\underset{2}{\bigcirc}} + 144\; {}_1\bigcirc\!\bigcirc{}_2 , \tag{2.67}$$

and subsequently to

$$\frac{\delta^2 W^{(2)}}{\delta 1\!-\!2\,\delta 3\!-\!4} = 288\; {}_3^1\!\!>\!\!<\!\!<\!{}_4^2 + 144\; {}_2^1\!\!>\!\!<\!\!<\!{}_4^3 + 288\; {}_2\!-\!\!\overset{1\,\bigcirc}{\underset{3}{+}}\!\!{}_4$$

$$+ 144\; {}_3\!-\!\!\overset{1\,\bigcirc}{\underset{4}{+}}\!\!{}_2 + 144\; {}_1\!-\!\!\overset{2\,\bigcirc}{\underset{3}{+}}\!\!{}_4 + 144\; {}_2^1\!\!\overset{\bigcirc}{\underset{\bigcirc}{}}{}_4^3 . \tag{2.68}$$

Inserting (2.67) and (2.68) into (2.61) and taking into account (2.65), we find the connected vacuum diagrams of order $p=3$ with their multiplicities as shown in Table I. We observe that the nonlinear operation in (2.61) does not lead to topologically new diagrams. It only corrects the multiplicities of the diagrams generated from the first two operations. This is true also in higher orders. The connected vacuum diagrams of the subsequent order $p=4$ and their multiplicities are listed in Table I.

As a crosscheck we can also determine the total multiplicities $M^{(p)}$ of all connected vacuum diagrams contributing to $W^{(p)}$. To this end we recall that each of the $M^{(p)}$ diagrams in $W^{(p)}$ consists of $2p$ lines. The amputation of one or two lines therefore leads to $2pM^{(p)}$ and $2p(2p-1)M^{(p)}$ diagrams with $2p-1$ and $2p-2$ lines, respectively. Considering only the total multiplicities, the graphical recursion relations (2.61) reduce to the form derived before in Ref. [7]

$$M^{(p+1)} = 16p(p+1)M^{(p)}$$

$$+ 16\sum_{q=1}^{p-1}\frac{p!}{(p-q-1)!(q-1)!}M^{(q)}M^{(p-q)}; \quad p \geq 1. \tag{2.69}$$

These are solved starting with the initial value

$$M^{(1)} = 3, \tag{2.70}$$

leading to the total multiplicities

$$M^{(2)} = 96, \; M^{(3)} = 9504, \; M^{(4)} = 1880064, \tag{2.71}$$

which agree with the results listed in Table I. In addition we note that the next orders would contain

$$M^{(5)} = 616108032, \; M^{(6)} = 301093355520,$$

$$M^{(7)} = 205062331760640 \qquad (2.72)$$

connected vacuum diagrams.

III. SCALAR $\phi^2 A$ THEORY

For the sake of generality, let us also study the situation where the quartic interaction of the ϕ^4 theory is generated by a scalar field A from a cubic $\phi^2 A$ interaction. The associated energy functional

$$E[\phi,A] = E^{(0)}[\phi,A] + E^{(\mathrm{int})}[\phi,A] \qquad (3.1)$$

decomposes into the free part

$$E^{(0)}[\phi,A] = \frac{1}{2}\int_{12} G_{12}^{-1}\phi_1\phi_2 + \frac{1}{2}\int_{12} H_{12}^{-1}A_1 A_2 \quad (3.2)$$

and the interaction

$$E^{(\mathrm{int})}[\phi,A] = \frac{\sqrt{g}}{2}\int_{123} V_{123}\phi_1\phi_2 A_3 . \qquad (3.3)$$

Indeed, as the field A appears only quadratically in (3.1), the functional integral for the partition function

$$Z = \int \mathcal{D}\phi\,\mathcal{D}A\, e^{-E[\phi,A]} \qquad (3.4)$$

can be exactly evaluated with respect to the field A, yielding

$$Z = \int \mathcal{D}\phi\ e^{-E^{(\mathrm{eff})}[\phi]} \qquad (3.5)$$

with the effective energy functional

$$E^{(\mathrm{eff})}[\phi] = -\frac{1}{2}\mathrm{Tr}\ln H^{-1} + \frac{1}{2}\int_{12} G_{12}^{-1}\phi_1\phi_2$$

$$-\frac{g}{8}\int_{123456} V_{125}V_{346}H_{56}\phi_1\phi_2\phi_3\phi_4 . \quad (3.6)$$

Apart from a trivial shift due to the negative free energy of the field A, the effective energy functional (3.6) coincides with that of a ϕ^4 theory in Eq. (2.1) with the quartic interaction

$$V_{1234} = -3\int_{56} V_{125}V_{346}H_{56} . \qquad (3.7)$$

If we supplement the previous Feynman rules (2.7), (2.9) by the free correlation function of the field A

$$\mathbf{1} \ \sim\!\sim\!\sim\ \mathbf{2} \quad \equiv \quad H_{\mathbf{12}} \qquad (3.8)$$

and the cubic interaction

$$\rangle\!\sim \quad \equiv \quad \int_{\mathbf{123}} V_{\mathbf{123}} , \qquad (3.9)$$

the intimate relation (3.7) between the ϕ^4-theory and the $\phi^2 A$- theory can be graphically illustrated by

$$(3.10)$$

This corresponds to a photon exchange in the so-called s, t, and u channels of Mandelstam's theory of the scattering matrix. Their infinite repetitions yield the relevant forces in the Hartree, Fock, and Bogoliubov approximations of many-body physics. In the following we analyze the $\phi^2 A$ theory along similar lines as before the ϕ^4 theory.

A. Perturbation theory

Expanding the exponential in the partition function (3.4) in powers of the coupling constant g, the resulting perturbation series reads

$$Z = \sum_{p=0}^{\infty} \frac{1}{(2p)!}\left(\frac{g}{4}\right)^p$$

$$\times \int \mathcal{D}\phi\,\mathcal{D}A\left(\int_{123456} V_{123}V_{456}\phi_1\phi_2\phi_4\phi_5 A_3 A_6\right)^p$$

$$\times e^{-E^{(0)}[\phi,A]} . \qquad (3.11)$$

Substituting the product of two fields ϕ or A by a functional derivative with respect to the kernels G^{-1} or H^{-1}, we conclude from (3.11)

$$Z = \sum_{p=0}^{\infty} \frac{(-2g)^p}{(2p)!}\left(\int_{123456} V_{123}V_{456}\frac{\delta^3}{\delta G_{12}^{-1}\delta G_{45}^{-1}\delta H_{36}^{-1}}\right)^p$$

$$\times e^{W^{(0)}} , \qquad (3.12)$$

where the zeroth order of the negative free energy reads

$$W^{(0)} = -\frac{1}{2}\mathrm{Tr}\ln G^{-1} - \frac{1}{2}\mathrm{Tr}\ln H^{-1} \equiv \frac{1}{2}\ \bigcirc\ + \frac{1}{2}\ \{\!\!\{\ \}\!\!\} . \qquad (3.13)$$

Inserting (3.13) in (3.12), the first-order contribution to the negative free energy yields

$$W^{(1)} = 2 \int_{123456} V_{123} V_{456} H_{36} G_{14} G_{25}$$

$$+ \int_{123456} V_{123} V_{456} H_{36} G_{12} G_{45}, \qquad (3.14)$$

which corresponds to the Feynman diagrams

$$W^{(1)} = 2 \quad \bowtie \quad + \quad \circ\!\!-\!\!\!\sim\!\!\!-\!\!\circ \quad . \qquad (3.15)$$

B. Functional differential equation for $W = \ln Z$

The derivation of a functional differential equation for the negative free energy W requires the combination of two independent steps. Consider first the identity

$$\int \mathcal{D}\phi \mathcal{D}A \, \frac{\delta}{\delta\phi_1} \{ \phi_2 e^{-E[\phi,A]} \} = 0, \qquad (3.16)$$

which immediately yields with the energy functional (3.1)

$$\delta_{12} Z + 2 \int_3 G_{13}^{-1} \frac{\delta Z}{\delta G_{23}^{-1}} + 2\sqrt{g} \int_{34} V_{134} \frac{\delta \{\langle A_4 \rangle Z\}}{\delta G_{23}^{-1}} = 0, \qquad (3.17)$$

where $\langle A \rangle$ denotes the expectation value of the field A. In order to close the functional differential equation, we consider the second identity

$$\int \mathcal{D}\phi \mathcal{D}A \, \frac{\delta}{\delta A_1} e^{-E[\phi,A]} = 0, \qquad (3.18)$$

which leads to

$$\langle A_1 \rangle Z = \sqrt{g} \int_{234} V_{234} H_{14} \frac{\delta Z}{\delta G_{23}^{-1}}. \qquad (3.19)$$

Inserting (3.19) in (3.17), we result in the desired functional differential equation for the negative free energy $W = \ln Z$:

$$\delta_{12} + 2 \int_2 G_{13}^{-1} \frac{\delta W}{\delta G_{23}^{-1}} = -2g \int_{34567} V_{134} V_{567}$$

$$\times H_{47} \left\{ \frac{\delta^2 W}{\delta G_{23}^{-1} \delta G_{56}^{-1}} + \frac{\delta W}{\delta G_{23}^{-1}} \frac{\delta W}{\delta G_{56}^{-1}} \right\}. \qquad (3.20)$$

A subsequent separation (2.54) of the zeroth-order (3.13) leads to a functional differential equation for the interaction part of the free energy $W^{(\mathrm{int})}$:

$$\int_{12} G_{12}^{-1} \frac{\delta W^{(\mathrm{int})}}{\delta G_{12}^{-1}} = -\frac{g}{4} \int_{123456} V_{123} V_{456} H_{36}$$

$$\times \{ G_{12} G_{45} + 2 G_{14} G_{25} \}$$

$$+ g \int_{123456} V_{123} V_{456} G_{12} H_{36} \frac{\delta W^{(\mathrm{int})}}{\delta G_{45}^{-1}}$$

$$- g \int_{123456} V_{123} V_{456} H_{36} \left\{ \frac{\delta^2 W^{(\mathrm{int})}}{\delta G_{12}^{-1} \delta G_{45}^{-1}} \right.$$

$$\left. + \frac{\delta W^{(\mathrm{int})}}{\delta G_{12}^{-1}} \frac{\delta W^{(\mathrm{int})}}{\delta G_{45}^{-1}} \right\}. \qquad (3.21)$$

Taking into account the functional chain rules (2.56), (2.57), the functional derivatives with respect to G^{-1} in (3.21) can be rewritten in terms of G:

$$\int_{12} G_{12} \frac{\delta W^{(\mathrm{int})}}{\delta G_{12}} = \frac{g}{4} \int_{123456} V_{123} V_{456} H_{36} \{ G_{12} G_{45} + 2 G_{14} G_{25} \}$$

$$+ g \int_{123456} V_{123} V_{456} H_{36} \{ G_{12} G_{47} G_{58}$$

$$+ 2 G_{14} G_{27} G_{58} \} \frac{\delta W^{(\mathrm{int})}}{\delta G_{78}}$$

$$+ g \int_{1234567891̄} V_{123} V_{456}$$

$$\times H_{36} G_{17} G_{28} G_{39} G_{41̄}$$

$$\times \left\{ \frac{\delta^2 W^{(\mathrm{int})}}{\delta G_{78} \delta G_{91̄}} + \frac{\delta W^{(\mathrm{int})}}{\delta G_{78}} \frac{\delta W^{(\mathrm{int})}}{\delta G_{91̄}} \right\}. \qquad (3.22)$$

C. Recursion relation and graphical solution

The functional differential equation (3.22) is now solved by the power series

$$W^{(\mathrm{int})} = \sum_{p=1}^{\infty} \frac{1}{(2p)!} \left(\frac{g}{4} \right)^p W^{(p)}. \qquad (3.23)$$

Using the property (2.33) that the coefficients $W^{(p)}$ satisfy the eigenvalue condition of the operator (2.32), we obtain both the recursion relation

$$W^{(p+1)} = 4(2p+1) \left\{ \int_{12345678} V_{123} V_{456} H_{36} (G_{12} G_{47} G_{58} \right.$$

$$+ 2 G_{14} G_{27} G_{58}) \frac{\delta W^{(p)}}{\delta G_{78}} + \int_{1234567891̄} V_{123} V_{456}$$

$$\times H_{36} G_{17} G_{28} G_{39} G_{41̄}$$

$$\left. \times \left[\frac{\delta^2 W^{(p)}}{\delta G_{78} \delta G_{91̄}} + \sum_{q=1}^{p-1} \binom{2p}{2q} \frac{\delta W^{(p-q)}}{\delta G_{78}} \frac{\delta W^{(q)}}{\delta G_{91̄}} \right] \right\} \qquad (3.24)$$

and the initial value (3.14). Using the Feynman rules (2.7), (3.8), and (3.9), the recursion relation (3.24) reads graphically

$$W^{(p+1)} = 4(2p+1)\left\{ \quad \frac{\delta W^{(p)}}{\delta 1 \text{---} 2} \quad {}_2^1 \!\!>\!\!\sim\!\!\bigcirc \quad + \, 2 \quad \frac{\delta W^{(p)}}{\delta 1 \text{---} 2} \quad {}_2^1 \text{---}\!\!\Big) \right.$$

$$+ \quad \frac{\delta^2 W^{(p)}}{\delta 1 \text{---} 2 \, \delta 3 \text{---} 4} \quad \begin{matrix} 1 \\ 2 \\ 3 \\ 4 \end{matrix}\!\!>\!\!\Big\} \quad + \quad \sum_{q=1}^{p-1} \binom{2p}{2q} \quad \frac{\delta W^{(p-q)}}{\delta 1 \text{---} 2} \quad {}_1^2 \!\!>\!\!\sim\!\!<\!\!{}_3^4 \quad \frac{\delta W^{(q)}}{\delta 3 \text{---} 4} \left. \right\}, \qquad p \geq 1,$$

$$\tag{3.25}$$

which is iterated starting from (3.15). In analogy to (2.64), this recursion relation can be cast in a closed diagrammatic way by using the alternative graphical rules (2.63):

$$\left(\!\!\boxed{p+1}\!\!\right) = 4(2p+1)\left\{ \bigcirc\!\!\sim\!\!<\!\!\boxed{p} \quad + \, 2 \, \boxed{}\!\!\boxed{p} \right.$$

$$+ \boxed{}\!\!\boxed{p} \quad + \, \sum_{q=1}^{p-1} \binom{2p}{2q} \boxed{p-q}\!\!>\!\!\sim\!\!<\!\!\boxed{q} \left. \right\}, \qquad p \geq 1. \tag{3.26}$$

We illustrate the procedure of solving the recursion relation (3.25) by constructing the three-loop vacuum diagrams. Applying one or two functional derivatives to (3.15), we have

$$\frac{\delta W^{(1)}}{\delta 1 \text{---} 2} = 2 \, {}_2^1\!\!>\!\!\sim\!\!\bigcirc \, + \, 4 \, {}_2^1\text{---}\!\!\Big) \,, \qquad \frac{\delta^2 W^{(1)}}{\delta 1 \text{---} 2 \, \delta 3 \text{---} 4} = 2 \, {}_1^2\!\!>\!\!\sim\!\!<\!\!{}_3^4 \, + \, 4 \, {}_3^1\!\!>\!\!\sim\!\!<\!\!{}_4^2 \,. \tag{3.27}$$

This is inserted into (3.25) to yield the three-loop diagrams shown in Table IV with their multiplicities. The table also contains the subsequent four-loop results, which we shall not derive here in detail. Observe that the multiplicity of a connected vacuum diagram in the $\phi^2 A$ theory is given by a formula similar to (2.10) in the ϕ^4 theory:

$$M_{\phi^2 A}^{E=0} = \frac{(2p)! \, 4^p}{2!^{S+D} N}. \tag{3.28}$$

Here S and D denote the number of self- and double connections, and N represents again the number of vertex permutations leaving the vacuum diagram unchanged.

The connected vacuum diagrams of the $\phi^2 A$ theory in Table IV can, of course, be converted to corresponding ones of the ϕ^4 theory in Table I, by shrinking wiggly lines to a point and dividing the resulting multiplicity by 3 in accordance with (3.10). This relation between connected vacuum diagrams in ϕ^4 and $\phi^2 A$ theory is emphasized by the numbering used in Table IV. For instance, the shrinking converts the five diagrams 4.1–4.5 in Table IV to the diagram 4 in Table I. Taking into account the different combinatorial factors in the expansion (2.6) and (3.23) as well as the factor 3 in the shrinkage (3.10), the multiplicity $M_{\phi^4}^{E=0}$ of a ϕ^4 diagram results from the corresponding one $M_{\phi^2 A}^{E=0}$ of the $\phi^2 A$ partner diagrams via the rule

$$M_{\phi^4}^{E=0} = \frac{1}{(2p-1)!!} M_{\phi^2 A}^{E=0}. \tag{3.29}$$

IV. COMPUTER GENERATION OF DIAGRAMS

Continuing the solution of the graphical recursion relations (2.61) and (3.25) to higher loops becomes an arduous task. We therefore automatize the procedure by computer algebra. Here we restrict ourselves to the ϕ^4 theory because of its relevance for critical phenomena.

A. Matrix representation of diagrams

To implement the procedure on a computer we must represent Feynman diagrams in the ϕ^4 theory by algebraic symbols. For this we use matrices as defined in Refs. [8–10]. Let p be the number of vertices of a given diagram and label them by indices from 1 to p. Set up an adjacency matrix $\mathbf{M}$ whose elements M_{ij} ($0 \leq i, j \leq p$) specify the number of lines joining the vertices i and j. The diagonal elements M_{ii} ($i > 0$) count the number of self-connections of the ith vertex. External lines of a diagram are labeled as if they were connected to a single additional dummy vertex with number 0. The matrix element M_{00} is set to zero by convention. The off-diagonal elements lie in the interval $0 \leq M_{ij} \leq 4$, while the diagonal elements for $i > 0$ are restricted by $0 \leq M_{ii} \leq 2$. We observe that the sum of the matrix elements M_{ij} in each but the zeroth row or column equals 4, where the diagonal elements count twice,

$$\sum_{j=0}^{p} M_{ij} + M_{ii} = \sum_{j=0}^{p} M_{ji} + M_{ii} = 4. \tag{4.1}$$

The matrix $\mathbf{M}$ is symmetric and is thus specified by

TABLE IV. Connected vacuum diagrams and their multiplicities of the $\phi^2 A$ theory up to four loops. Each diagram is characterized by the vector $(S, D; N)$ whose components specify the number of self- and double connections as well as the vertex permutations leaving the vacuum diagram unchanged, respectively.

p	$W^{(p)}$
1	#1.1 2 (0,1;2) #1.2 1 (2,0;2)
2	#2.1 48 (0,0;8) #2.2 24 (0,2;4) #3.1 96 (0,0;4) #3.2 96 (1,0;2) #3.3 24 (2,1;2)
3	#4.1 3840 (0,0;12) #4.2 11520 (0,0;4) #4.3 3840 (0,0;12) #4.4 960 (0,3;6) #4.5 5760 (0,1;4) #5.1 11520 (0,1;2) #5.2 23040 (0,0;2) #5.3 11520 (1,0;2) #5.4 5760 (1,1;2) #6.1 7680 (0,0;6) #6.2 11520 (1,0;2) #6.3 5760 (2,0;2) #6.4 960 (3,0;6) #7.1 11520 (0,0;4) #7.2 5760 (0,0;8) #7.3 11520 (1,0;2) #7.4 5760 (1,1;2) #7.5 1440 (2,2;2) #7.6 2880 (2,0;4)

$(p+1)(p+2)/2-1$ elements. Each matrix characterizes a unique diagram and determines its multiplicity via formula (2.28). From the matrix $\mathbf{M}$ we read off directly the number of self-, double, triple, fourfold connections S, D, T, F and the number of external legs $E = \Sigma_{i=1}^{p} M_{0i}$. It also permits us to calculate the number N. For this we observe that the matrix $\mathbf{M}$ is not unique, since so far the vertex numbering is arbitrary. In fact, N is the number of combined permutations of vertices and external lines that leave the matrix $\mathbf{M}$ unchanged [compare to the statement after (2.28)]. If n_M denotes the number of different matrices representing the same diagram, the number N is given by

$$N = \frac{p!}{n_M} \prod_{i=1}^{p} M_{0i}!, \qquad (4.2)$$

where the matrix elements M_{0i} count the number of external legs connected to the ith vertex. One way to determine the number n_M is to repeatedly perform the $p(p-1)/2$ exchanges of pairs of rows and columns except the zeroth ones, until no new matrix is generated anymore. For larger matrices this way of determining n_M is quite tedious. Below we will give a better approach. Inserting Eq. (4.2) into the formula (2.28), we obtain the multiplicity of the diagram represented by $\mathbf{M}$. This may be used to crosscheck the multiplicities obtained before when solving the graphical recursion relation (2.61).

So far, the vertex numbering has been arbitrary, making the matrix representation of a diagram nonunique. To achieve uniqueness, we customize to our problem the procedure introduced in [11]. First we group the vertices in a given diagram into different classes, which are defined by the four tuples (E, S, D, T) containing the number of external legs, self-, double, and triple connections of a vertex. The classes are sorted by increasing numbers of E, then S, then D, then T. In general, there can still be vertices that coincide in all four numbers and whose ordering is therefore still arbitrary. To achieve unique ordering among these vertices, we associate with each matrix a number whose digits are composed of the matrix elements $M_{ij}(0 \leq j \leq i \leq p)$, i.e., we form the number with the $(p+1)(p+2)/2-1$ elements

$$M_{10}M_{11}|M_{20}M_{21}M_{22}|M_{30}M_{31}M_{32}M_{33}|...M_{pp}. \quad (4.3)$$

To guide the eye, we have separated the digits stemming from different rows by vertical lines. The smallest of these numbers compatible with the vertex ordering introduced above is chosen to represent the diagram uniquely. Instead we could have also allowed all vertex permutations and identified the number (4.3) with a unique representation of a given diagram. However, for most diagrams containing several vertices, this would drastically inflate the number of admissible matrices and therefore the effort for finding a unique representation.

Now we can also give an improved procedure for finding n_M. Let n_M' be the number of different matrices compatible with the vertex ordering by the four tuples introduced above. Let there be c classes of vertices and $k_1, ..., k_c$ vertices belonging to each class. Then we have

$$n_M = \frac{p!}{\prod_{j=1}^{c} k_j!} n_M' \qquad (4.4)$$

or, together with (4.2),

$$N = \frac{1}{n'_M} \left(\prod_{j=1}^{c} k_j! \right) \left(\prod_{i=1}^{p} M_{0i}! \right). \qquad (4.5)$$

As an example, consider the following diagram of the four-point function with $p=3$ vertices:

$$\qquad (4.6)$$

Its vertices are grouped into $c=2$ classes with $k_1=2$ vertices belonging to the first class characterized by the four tuple $(E,S,D,T)=(1,0,1,0)$ and $k_2=1$ vertex belonging to the second class $(E,S,D,T)=(2,0,0,0)$. When labeling the vertices in view of the unique matrix representation, the vertex in the second class comes last because of the higher number of external legs. Exchanging the other two vertices in the first class does not change the adjacency matrix anymore due to the reflection symmetry of the diagram (4.6). Thus its unique matrix representation reads

$$\begin{pmatrix} 0 & 1 & 1 & 2 \\ 1 & 0 & 2 & 1 \\ 1 & 2 & 0 & 1 \\ 2 & 1 & 1 & 0 \end{pmatrix}, \qquad (4.7)$$

with rows and columns indexed from 0 to 3. According to Eq. (4.3), the matrix (4.7) yields the number

$$10|120|2110. \qquad (4.8)$$

As there is $n'_m=1$ matrix compatible with the vertex ordering by the four tuples, the number N of vertex permutations of the diagram (4.6) is determined from (4.5) as 4 (compare the corresponding entry in Table III).

A more complicated example is provided by the following diagram of the two-point function with $p=4$ vertices:

$$\qquad (4.9)$$

Here we have again $c=2$ classes, the first one is $(E,S,D,T)=(0,0,2,0)$ with $k_1=2$ vertices and the second one $(E,S,D,T)=(1,0,1,0)$ with $k_2=2$ vertices. Exchanging both vertices in each class leads now to $n'_M=2$ different matrices

$$\begin{pmatrix} 0 & 0 & 0 & 1 & 1 \\ 0 & 0 & 2 & 2 & 0 \\ 0 & 2 & 0 & 0 & 2 \\ 1 & 2 & 0 & 0 & 1 \\ 1 & 0 & 2 & 1 & 0 \end{pmatrix}, \begin{pmatrix} 0 & 0 & 0 & 1 & 1 \\ 0 & 0 & 2 & 0 & 2 \\ 0 & 2 & 0 & 2 & 0 \\ 1 & 0 & 2 & 0 & 1 \\ 1 & 2 & 0 & 1 & 0 \end{pmatrix}.$$

$$\qquad (4.10)$$

For the unique matrix representation we have to choose the last matrix as it leads to the smaller number

$$00|020|1020|12010. \qquad (4.11)$$

From Eq. (4.5) we read off that the number N of vertex permutations of the diagram (4.9) is 2 (compare the corresponding entry in Table II).

The matrix $\mathbf{M}$ contains, of course, all information on the topological properties of a diagram [9,10]. For this we define the submatrix $\tilde{\mathbf{M}}$ by removing the zeroth row and column from $\mathbf{M}$. This allows us to recognize the connectedness of a diagram: A diagram is disconnected if there is a vertex numbering for which $\tilde{\mathbf{M}}$ is a block matrix. Furthermore a vertex is a cut vertex, i.e., a vertex which links two otherwise disconnected parts of a diagram, if the matrix $\tilde{\mathbf{M}}$ has an almost block form for an appropriate numbering of vertices in which the blocks overlap only on some diagonal element $\tilde{M}_{ii}$, i.e., the matrix $\tilde{\mathbf{M}}$ takes block form if the ith row and column are removed. Similarly, the matrix $\tilde{\mathbf{M}}$ allows us to recognize a one-particle-reducible diagram, which falls into two pieces by cutting a certain line. Removing a line amounts to reducing the associated matrix elements in the submatrix $\tilde{\mathbf{M}}$ by one. If the resulting matrix $\tilde{\mathbf{M}}$ has block form for a certain vertex ordering, the diagram is one-particle reducible.

B. Practical generation

We are now prepared for the computer generation of Feynman diagrams. First the vacuum diagrams are generated from the recursion relation (2.61). From these the diagrams of the connected two- and four-point functions are obtained by cutting or removing lines. We used a MATHEMATICA program to perform this task. The resulting unique matrix representations of the diagrams up to the order $p=4$ are listed in Tables V–VII. They are the same as those derived before by hand in Tables I–III. Higher-order results up to $p=6$, containing all diagrams that are relevant for the five-loop renormalization of ϕ^4 theory in $d=4-\epsilon$ dimensions [10,20], are made available on the internet [19], where also the program can be found.

1. Connected vacuum diagrams

The computer solution of the recursion relation (2.61) necessitates to keep an exact record of the labeling of external legs of intermediate diagrams which arise from differentiating a vacuum diagram with respect to a line once or twice. To this end we have to extend our previous matrix representation of diagrams where the external legs are labeled as if they were connected to a simple additional vertex with number 0. For each matrix representing a diagram we define an associated vector that contains the labels of the external legs connected to each vertex. This vector has the length of the dimension of the matrix and will be added to the matrix as an extra left column, separated by a vertical line. Consider, as an example, the diagram (4.6) of the four-point function with $p=3$ vertices, where the spatial indices 1, 2, 3, 4 are assigned in a particular order:

$$\qquad (4.12)$$

In our extended matrix notation, such a diagram can be represented in total by six matrices:

TABLE V. Unique matrix representation of all connected vacuum diagrams of ϕ^4 theory up to the order $p=4$. The number in the first column corresponds to their graphical representation in Table I. The matrix elements M_{ij} represent the numbers of lines connecting two vertices i and j, omitting $M_{i0}=0$ for simplicity. The running numbers of the vertices are listed on top of each column in the first two rows. The further columns contain the vector $(S, D, T, F; N)$ characterizing the topology of the diagram, the multiplicity M, and the weight $W=M/[(4!)^p p!]$. The graphs are ordered according to their number of self-connections, then double connections, then triple connections, then fourfold connections, then the number (4.3).

$W^{(1)}$: 1 diagram

i	1		
j	1		
#	M_{ij}	$(S,D,T,F;N)$	M	W
1	2	(2,1,0,0;1)	3	1/8

$W^{(2)}$: 2 diagrams

i	1	22		
j	1	12		
#	M_{ij}		$(S,D,T,F;N)$	M	W
2	0	40	(0,0,0,1;2)	24	1/48
3	1	21	(2,1,0,0;2)	72	1/16

$W^{(3)}$: 4 diagrams

i	1	22	333		
j	1	12	123		
#	M_{ij}			$(S,D,T,F;N)$	M	W
4	0	20	220	(0,3,0,0;6)	1728	1/48
5	0	30	111	(1,0,1,0;2)	3456	1/24
7	0	21	201	(2,2,0,0;2)	2592	1/32
6	1	11	111	(3,0,0,0;6)	1728	1/48

$W^{(4)}$: 10 diagrams

i	1	22	333	4444		
j	1	12	123	1234		
#	M_{ij}				$(S,D,T,F;N)$	M	W
10	0	00	130	3100	(0,0,2,0;4)	55296	1/144
9	0	10	120	2110	(0,2,0,0;8)	248832	1/32
8	0	00	220	2200	(0,4,0,0;8)	62208	1/128
14	0	30	110	0021	(1,1,1,0;2)	165888	1/48
11	0	10	220	1101	(1,2,0,0;2)	497664	1/16
12	0	30	011	1011	(2,0,1,0;2)	165888	1/48
13	0	20	111	1101	(2,1,0,0;4)	248832	1/32
17	0	20	021	2001	(2,3,0,0;2)	124416	1/64
15	0	11	111	2001	(3,1,0,0;2)	248832	1/32
16	1	01	111	1101	(4,0,0,0;8)	62208	1/128

$$
\begin{pmatrix} \{\,\} & 0 & 2 & 1 & 1 \\ \{1,2\} & 2 & 0 & 1 & 1 \\ \{3\} & 1 & 1 & 0 & 2 \\ \{1\} & 1 & 1 & 2 & 0 \end{pmatrix},\quad
\begin{pmatrix} \{\,\} & 0 & 1 & 2 & 1 \\ \{3\} & 1 & 0 & 1 & 2 \\ \{1,2\} & 2 & 1 & 0 & 1 \\ \{4\} & 1 & 2 & 1 & 0 \end{pmatrix},\quad
\begin{pmatrix} \{\,\} & 0 & 1 & 1 & 2 \\ \{3\} & 1 & 0 & 2 & 1 \\ \{4\} & 1 & 2 & 0 & 1 \\ \{1,2\} & 2 & 1 & 1 & 0 \end{pmatrix},
$$

$$
\begin{pmatrix} \{\,\} & 0 & 2 & 1 & 1 \\ \{1,2\} & 2 & 0 & 1 & 1 \\ \{4\} & 1 & 1 & 0 & 2 \\ \{3\} & 1 & 1 & 2 & 0 \end{pmatrix},\quad
\begin{pmatrix} \{\,\} & 0 & 1 & 2 & 1 \\ \{4\} & 1 & 0 & 1 & 2 \\ \{1,2\} & 2 & 1 & 0 & 1 \\ \{3\} & 1 & 2 & 1 & 0 \end{pmatrix},\quad
\begin{pmatrix} \{\,\} & 0 & 1 & 1 & 2 \\ \{4\} & 1 & 0 & 2 & 1 \\ \{3\} & 1 & 2 & 0 & 1 \\ \{1,2\} & 2 & 1 & 1 & 0 \end{pmatrix}. \tag{4.13}
$$

When constructing of the vacuum diagrams from the recursion relation (2.61), starting from the two-loop diagram (2.62), we have to represent three different elementary operations in our extended matrix notation:

(i) Taking one or two derivatives of a vacuum diagram with respect to a line. For example, we apply this operation to the vacuum diagram 2 in Table I

TABLE VI. Unique matrix representation of all diagrams of the connected two-point function of ϕ^4 theory up to the order $p=4$. The numbers in the first column correspond to their graphical representation in Table II. The matrix elements M_{ij} represent the numbers of lines connecting two vertices i and j. The running numbers of the vertices are listed on top of each column in the first two rows. The further columns contain the vector $(S, D, T; N)$ characterizing the topology of the diagram, the multiplicity M, and the weight $W = M/[(4!)^p p!]$. The graphs are ordered according to their number of self-connections, then double connections, then triple connections, then the number (4.3).

$G_{12}^{(1)}$: 1 diagram

i	11			
j	01			
#	M_{ij}	$(S,D,T;N)$	M	W
1.1	21	(1,0,0;2)	12	1/2

$G_{12}^{(2)}$: 3 diagrams

i	11	222			
j	01	012			
#	M_{ij}		$(S,D,T;N)$	M	W
2.1	10	130	(0,0,1;2)	192	1/6
3.1	01	220	(1,1,0;2)	288	1/4
3.2	11	111	(2,0,0;2)	288	1/4

$G_{12}^{(3)}$: 8 diagrams

i	11	222	3333			
j	01	012	0123			
#	M_{ij}			$(S,D,T;N)$	M	W
5.1	00	030	2110	(0,0,1;4)	6912	1/12
4.1	00	120	1210	(0,2,0;2)	20736	1/4
5.3	00	130	1101	(1,0,1;1)	13824	1/6
5.2	01	110	1120	(1,1,0;2)	20736	1/4
7.1	00	021	2200	(1,2,0;2)	10368	1/8
6.1	01	011	2110	(2,0,0;4)	10368	1/8
7.2	01	120	1011	(2,1,0;1)	20736	1/4
6.2	01	111	1101	(3,0,0;2)	10368	1/8

$G_{12}^{(4)}$: 30 diagrams

i	11	222	3333	44444			
j	01	012	0123	01234			
#	M_{ij}				$(S,D,T;N)$	M	W
10.1	00	010	1030	13000	(0,0,2;2)	221184	1/36
9.1	00	020	1110	11110	(0,1,0;4)	1990656	1/4
14.4	00	030	0110	20020	(0,1,1;4)	331776	1/24
10.2	00	030	1010	11020	(0,1,1;2)	663552	1/12
11.1	00	010	0220	21100	(0,2,0;4)	995328	1/8
9.2	00	010	1120	12100	(0,2,0;2)	1990656	1/4
8.1	00	020	1020	12010	(0,3,0;2)	995328	1/8
12.4	00	030	0011	21010	(1,0,1;2)	663552	1/12
14.3	00	030	1110	10011	(1,0,1;2)	663552	1/12
13.2	00	020	0111	21100	(1,1,0;4)	995328	1/8
11.4	00	011	1110	12010	(1,1,0;1)	3981312	1/2
14.2	00	001	1300	11200	(1,1,1;1)	663552	1/12
11.3	00	001	1210	12100	(1,2,0;2)	995328	1/8
11.2	00	020	1120	11001	(1,2,0;1)	1990656	1/4
14.1	00	021	1100	11020	(1,2,0;2)	995328	1/8
17.1	00	020	0021	22000	(1,3,0;2)	497664	1/16
13.1	01	001	1110	11110	(2,0,0;4)	995328	1/8
12.3	00	011	1300	10101	(2,0,1;1)	663552	1/12
12.2	00	030	1011	11001	(2,0,1;2)	331776	1/24
15.3	00	011	0111	22000	(2,1,0;4)	497664	1/16
15.4	00	011	0201	21100	(2,1,0;2)	995328	1/8
13.3	00	011	1210	11001	(2,1,0;1)	1990656	1/4
12.1	01	011	1010	11020	(2,1,0;2)	995328	1/8
17.2	00	021	1200	10011	(2,2,0;1)	995328	1/8
17.3	01	001	1020	12010	(2,2,0;2)	497664	1/16
16.1	01	001	0111	21100	(3,0,0;4)	497664	1/16
15.5	01	011	1110	10011	(3,0,0;2)	995328	1/8
15.2	00	021	1101	11001	(3,1,0;2)	497664	1/16
15.1	01	001	1120	11001	(3,1,0;1)	995328	1/8
16.2	01	011	1011	11001	(4,0,0;2)	497664	1/16

$$\frac{\delta^2}{\delta G_{12} \delta G_{34}} \bigcirc = 2 \frac{\delta}{\delta G_{12}} \left[3 -\!\bigcirc\!- 4 \;+\; 4 -\!\bigcirc\!- 3 \right]$$

$$= 3 \left[\begin{array}{c}1\\3\end{array}\!\!\times\!\!\bigcirc\!\!\times\!\!\begin{array}{c}2\\4\end{array} + \begin{array}{c}2\\3\end{array}\!\!\times\!\!\bigcirc\!\!\times\!\!\begin{array}{c}1\\4\end{array} + \begin{array}{c}1\\4\end{array}\!\!\times\!\!\bigcirc\!\!\times\!\!\begin{array}{c}2\\3\end{array} + \begin{array}{c}2\\4\end{array}\!\!\times\!\!\bigcirc\!\!\times\!\!\begin{array}{c}1\\3\end{array} \right]. \qquad (4.14)$$

This has the matrix representation

$$\frac{\delta^2}{\delta G_{12}\delta G_{34}}\begin{pmatrix} \{\} & 0 & 0 & 0\\ \{\} & 0 & 0 & 4\\ \{\} & 0 & 4 & 0 \end{pmatrix} = 2\frac{\delta}{\delta G_{12}}\left[\begin{pmatrix} \{\} & 0 & 1 & 1\\ \{3\} & 1 & 0 & 3\\ \{4\} & 1 & 3 & 0 \end{pmatrix} + \begin{pmatrix} \{\} & 0 & 1 & 1\\ \{4\} & 1 & 0 & 3\\ \{3\} & 1 & 3 & 0 \end{pmatrix} \right]$$

$$= 3\left[\begin{pmatrix} \{\} & 0 & 2 & 2\\ \{1,3\} & 2 & 0 & 2\\ \{2,4\} & 2 & 2 & 0 \end{pmatrix} + \begin{pmatrix} \{\} & 0 & 2 & 2\\ \{2,3\} & 2 & 0 & 2\\ \{1,4\} & 2 & 2 & 0 \end{pmatrix} + \begin{pmatrix} \{\} & 0 & 2 & 2\\ \{1,4\} & 2 & 0 & 2\\ \{2,3\} & 2 & 2 & 0 \end{pmatrix} \right.$$

$$\left. + \begin{pmatrix} \{\} & 0 & 2 & 2\\ \{2,4\} & 2 & 0 & 2\\ \{1,3\} & 2 & 2 & 0 \end{pmatrix} \right]. \qquad (4.15)$$

The first and fourth matrix as well as the second and third matrix represent the same diagram in (4.14), as can be seen by permuting rows and columns of either matrix.

(ii) Combining two or three diagrams to one. We perform this operation by creating a block matrix of internal lines from the submatrices representing the internal lines of the original diagrams. Then the zeroth row or column is added to represent the respective original external spatial arguments. Let us illustrate the combination of two diagrams by the example

$$
\equiv
\begin{pmatrix}
\{\} & 0\ 1\ 1 \\
\{1\} & 1\ 0\ 3 \\
\{2\} & 1\ 3\ 0
\end{pmatrix}
\begin{pmatrix}
\{\} & 0\ 2 \\
\{1,2\} & 2\ 1
\end{pmatrix}
\rightarrow
\begin{pmatrix}
\{\} & 0\ 2\ 1\ 1 \\
\{1,2\} & 2\ 1\ 0\ 0 \\
\{1\} & 1\ 0\ 0\ 3 \\
\{2\} & 1\ 0\ 3\ 0
\end{pmatrix}
$$

(4.16)

and the combination of three diagrams by

$$
\begin{pmatrix}
\{\} & 0\ 2 \\
\{1,2\} & 2\ 1
\end{pmatrix}
\begin{pmatrix}
\{\} & 0\ 4 \\
\{1,2,3,4\} & 4\ 0
\end{pmatrix}
\begin{pmatrix}
\{\} & 0\ 2 \\
\{3,4\} & 2\ 1
\end{pmatrix}
\rightarrow
\begin{pmatrix}
\{\} & 0\ 2\ 4\ 2 \\
\{1,2\} & 2\ 1\ 0\ 0 \\
\{1,2,3,4\} & 4\ 0\ 0\ 0 \\
\{3,4\} & 2\ 0\ 0\ 1
\end{pmatrix}.
$$

(4.17)

We observe that the ordering of the submatrices in the block matrix is arbitrary at this point; we just have to make sure to distribute the spatial labels of the external legs correctly.

(iii) Connecting external legs with the same label and creating an internal line. This is achieved in our extended matrix notation by eliminating the spatial labels of external legs that appear twice, and by performing an appropriate entry in the matrix for the additional line. Thus we obtain, for instance, from (4.16)

$$
\equiv
\begin{pmatrix}
\{\} & 0\ 0\ 0\ 0 \\
\{\} & 0\ 1\ 1\ 1 \\
\{\} & 0\ 1\ 0\ 3 \\
\{\} & 0\ 1\ 3\ 0
\end{pmatrix}
$$

(4.18)

and similarly from (4.17)

$$
\equiv
\begin{pmatrix}
\{\} & 0\ 0\ 0\ 0 \\
\{\} & 0\ 1\ 2\ 0 \\
\{\} & 0\ 2\ 0\ 2 \\
\{\} & 0\ 0\ 2\ 1
\end{pmatrix}.
$$

(4.19)

As we reobtain at this stage connected vacuum diagrams where there are no more external legs to be labeled, we may omit the extra left column of the matrices.

The selection of a unique matrix representation for the resulting vacuum diagrams obtained at each stage of the recursion relation proceeds as explained in detail in Sec. IV A. By comparing we find out which of the vacuum diagrams are topologically identical and sum up their individual multiplicities. Along these lines, the recursion relation (2.61) is solved by a MATHEMATICA program up to the order $p=6$. The results are shown in Table V and in Ref. [19]. To each order p, the numbers $n_p^{(0)}$ of topologically different con-

nected vacuum diagrams are

$$
\begin{array}{|c||c|c|c|c|c|c|}
\hline
p & 1 & 2 & 3 & 4 & 5 & 6 \\
\hline
n_p^{(0)} & 1 & 2 & 4 & 10 & 28 & 97 \\
\hline
\end{array}
\tag{4.20}
$$

A direct comparison with other, already established computer programs like FEYNARTS [1–3] or QGRAF [4,5] shows that the automatization of the graphical recursion relation (2.61) in terms of our MATHEMATICA code is inefficient. According to our experience, the major part of the CPU time needed for the generation of high-loop order diagrams is devoted to the reordering of vertices to obtain the unique matrix representation of a diagram—a problem faced also by other graph-generating methods. After implementation of a dedicated algorithm for the vertex ordering written for instance in Fortran or C, we would therefore expect CPU times

for the time-consuming high-loop diagrams which are comparable to those of other programs.

2. Two- and four-point functions G_{12} and G^c_{1234} from cutting lines

Having found all connected vacuum diagrams, we derive from these the diagrams of the connected two- and four-point functions by using the relations (2.18) and (2.25). In the matrix representation, cutting a line is essentially identical to removing a line as explained above, except that we now interpret the labels that represent the external spatial labels as sitting on the end of lines. Since we are not going to distinguish between trivially "crossed" diagrams that are related by exchanging external labels in our computer implementation, we need no longer carry around external spatial labels. Thus we omit the extra left column of the matrix representing a diagram when generating vacuum diagrams. As an example, consider cutting a line in diagram 3 in Table I

$$
-\frac{\delta}{\delta G^{-1}}
\begin{pmatrix}
0 & 0 & 0 \\
0 & 1 & 2 \\
0 & 2 & 1
\end{pmatrix}
= 2
\begin{pmatrix}
0 & 1 & 1 \\
1 & 1 & 1 \\
1 & 1 & 1
\end{pmatrix}
+
\begin{pmatrix}
0 & 2 & 0 \\
2 & 0 & 2 \\
0 & 2 & 1
\end{pmatrix}
+
\begin{pmatrix}
0 & 0 & 2 \\
0 & 1 & 2 \\
2 & 2 & 0
\end{pmatrix}.
\tag{4.22}
$$

which has the matrix representation

Here the plus signs and multiplication by 2 have a set theoretical meaning and are not to be understood as matrix algebra operations. The last two matrices represent, incidentally, the same diagram in (4.21) as can be seen by exchanging the last two rows and columns of either matrix.

To create the connected four-point function, we also have to consider second derivatives of vacuum diagrams with respect to G^{-1}. If an external line is cut, an additional external line will be created, which is not connected to any vertex. It can be interpreted as a self-connection of the zeroth vertex, which collects the external lines. This may be accommodated in the matrix notation by letting the matrix element M_{00} count the number of lines not connected to any vertex. For example, taking the derivative of the first diagram in Eq. (4.21) gives

with the matrix notation

$$
-\frac{\delta}{\delta G^{-1}}
\begin{pmatrix}
0 & 1 & 1 \\
1 & 1 & 1 \\
1 & 1 & 1
\end{pmatrix}
=
\begin{pmatrix}
0 & 3 & 1 \\
3 & 0 & 1 \\
1 & 1 & 1
\end{pmatrix}
+
\begin{pmatrix}
0 & 1 & 3 \\
1 & 1 & 1 \\
3 & 1 & 0
\end{pmatrix}
$$
$$
+
\begin{pmatrix}
0 & 2 & 2 \\
2 & 1 & 0 \\
2 & 0 & 1
\end{pmatrix}
+ 2
\begin{pmatrix}
1 & 1 & 1 \\
1 & 1 & 1 \\
1 & 1 & 1
\end{pmatrix}.
\tag{4.24}
$$

The first two matrices represent the same diagram as can be seen from Eq. (4.23). The last two matrices in Eq. (4.24) correspond to disconnected diagrams: the first one because of the absence of a connection between the two vertices, the second one because of the disconnected line represented by the entry $M_{00}=1$. In the full expression for the two-loop contribution $G^{c,(2)}_{1234}$ to the four-point function in Eq. (2.25) all disconnected diagrams arising from cutting a line in $G^{(2)}_{12}$ are canceled by diagrams resulting from the sum. Therefore we may omit the sum, take only the first term and discard all disconnected diagrams it creates. This is particularly useful for treating low orders by hand. If we include the sum, we use the prescription of combining diagrams into one as de-

TABLE VII. Unique matrix representation of all diagrams of the connected four-point function of ϕ^4 theory up to the order $p=4$. The numbers in the first column correspond to their graphical representation in Table III. The matrix elements M_{ij} represent the numbers of lines connecting two vertices i and j. The running numbers of the vertices are listed on top of each column in the first two rows. The further columns contain the vector $(S,D,T;N)$ characterizing the topology of the diagram, the multiplicity M, and the weight $W=M/[(4!)^p p!]$. The graphs are ordered according to their number of self-connections, then double connections, then triple connections, then the number (4.3).

$\boldsymbol{G}^{c,(1)}_{1234}$: 1 diagram

i	11			
j	01			
#	M_{ij}	$(S,D,T;N)$	M	W
1.1.1	40	(0,0,0;24)	24	1

$\boldsymbol{G}^{c,(2)}_{1234}$: 2 diagrams

i	11	222			
j	01	012			
#	M_{ij}		$(S,D,T;N)$	M	W
2.1.1, 3.1.1	20	220	(0,1,0;8)	1728	3/2
3.1.2, 3.2.1	11	310	(1,0,0;6)	2304	2

$\boldsymbol{G}^{c,(3)}_{1234}$: 8 diagrams

i	11	222	3333			
j	01	012	0123			
#	M_{ij}			$(S,D,T;N)$	M	W
5.1.2, 5.3.2	00	130	3100	(0,0,1;6)	55296	2/3
4.1.2, 5.1.1, 5.2.1	10	120	2110	(0,1,0;4)	248832	3
4.1.1, 7.1.1	00	220	2200	(0,2,0;8)	62208	3/4
5.2.2, 6.1.1	01	210	2110	(1,0,0;8)	124416	3/2
7.1.3, 7.2.3	01	120	3010	(1,1,0;6)	82944	1
5.2.3, 5.3.1, 7.1.2, 7.2.1	10	111	2200	(1,1,0;2)	248832	3
6.1.3, 6.2.1	01	111	3100	(2,0,0;6)	82944	1
6.1.2, 6.2.2, 7.2.2	11	101	2110	(2,0,0;4)	124416	3/2

$\boldsymbol{G}^{c,(4)}_{1234}$: 37 diagrams

i	11	222	3333	44444			
j	01	012	0123	01234			
#	M_{ij}				$(S,D,T;N)$	M	W
9.1.2	10	110	1110	11110	(0,0,0;24)	7962624	1
10.2.2, 12.4.1	00	030	2010	21010	(0,0,1;8)	3981312	1/2
14.3.1, 14.4.1	00	030	1110	30010	(0,0,1;12)	2654208	1/3
9.1.1, 13.2.1	00	020	2110	21100	(0,1,0;16)	5971968	3/4
9.1.3, 9.2.3, 11.1.1, 11.4.1	00	110	1210	21100	(0,1,0;2)	47775744	6
10.1.1, 10.2.3, 14.2.1, 14.4.2	00	130	1100	20020	(0,1,1;2)	7962624	1
11.1.3, 11.2.1	00	020	1120	31000	(0,2,0;6)	7962624	1
9.2.2, 14.1.1, 14.4.3	00	110	1120	22000	(0,2,0;4)	11943936	3/2
8.1.3, 11.1.2, 11.3.1	00	120	1200	20110	(0,2,0;4)	11943936	3/2
8.1.2, 9.2.1, 10.2.1	10	100	1120	12100	(0,2,0;4)	11943936	3/2
8.1.1, 17.1.1	00	020	2020	22000	(0,3,0;8)	2985984	3/8
11.4.6, 13.1.1, 13.2.3	01	110	1110	20110	(1,0,0;4)	23887872	3
12.3.1, 12.4.4	00	011	1300	30100	(1,0,1;6)	2654208	1/3
12.2.1, 12.4.2	00	030	1011	31000	(1,0,1;6)	2654208	1/3
12.3.2, 12.4.3, 14.2.2, 14.3.2	00	130	1001	21010	(1,0,1;2)	7962624	1
11.4.5, 15.3.1, 15.4.1	00	011	2110	22000	(1,1,0;4)	11943936	3/2
14.1.4, 15.4.4	00	021	2100	21010	(1,1,0;8)	5971968	3/4
13.2.4, 13.3.5	00	011	1210	31000	(1,1,0;6)	7962624	1
11.2.3, 11.4.2, 13.2.2, 13.3.1	00	120	1101	21100	(1,1,0;2)	23887872	3
11.3.3, 11.4.4, 12.1.1, 12.4.5	01	100	1120	21100	(1,1,0;2)	23887872	3
11.2.2, 11.4.3, 14.1.2, 14.3.3	10	110	1120	11001	(1,1,0;2)	23887872	3
17.1.4, 17.2.4	00	021	1200	30010	(1,2,0;6)	3981312	1/2
11.2.4, 11.3.2, 17.1.2, 17.2.1	00	120	1011	22000	(1,2,0;2)	11943936	3/2
14.1.3, 14.2.3, 17.1.3, 17.3.1	01	100	1210	20200	(1,2,0;2)	11943936	3/2
13.1.3, 16.1.1	01	001	2110	21100	(2,0,0;16)	2985984	3/8
12.1.3, 16.1.2	01	011	2010	21010	(2,0,0;8)	5971968	3/4
15.3.4, 15.5.4	01	011	1110	30010	(2,0,0;12)	3981312	1/2
13.1.2, 13.3.4, 15.4.2, 15.5.1	01	110	1011	21100	(2,0,0;2)	23887872	3
15.2.3, 15.4.6	00	021	1101	31000	(2,1,0;6)	3981312	1/2
15.1.4, 15.4.5	01	001	1120	31000	(2,1,0;6)	3981312	1/2
13.3.2, 15.2.1, 15.3.3	00	111	1101	22000	(2,1,0;4)	5971968	3/4
12.1.4, 12.3.3, 15.1.1, 15.3.2	01	110	1101	20200	(2,1,0;2)	11943936	3/2
15.1.3, 15.4.3, 17.2.3, 17.3.2	01	120	1001	20110	(2,1,0;2)	11943936	3/2
12.1.2, 12.2.2, 13.3.3, 17.2.2	10	120	1011	11001	(2,1,0;2)	11943936	3/2
16.1.4, 16.2.1	01	011	1011	31000	(3,0,0;6)	3981312	1/2
15.1.2, 15.5.3, 16.1.3, 16.2.2	01	101	1101	21100	(3,0,0;2)	11943936	3/2
15.2.2, 15.5.2	10	111	1101	11001	(3,0,0;6)	3981312	1/2

scribed above in Sec. IV B, except that we now omit the extra vector with the labels of spatial arguments.

3. Two- and four-point functions G_{12} and G^c_{1234} from removing lines

Instead of cutting lines of connected vacuum diagrams once or twice, the perturbative coefficients of $\mathbf{G}_{12}$ and $\mathbf{G}^c_{1234}$ can also be obtained graphically by removing lines. Indeed, from (2.16), (2.44), (2.54), and (2.56) we get for the two-point function

$$\mathbf{G}_{12}=G_{12}+2\int_{34}G_{13}G_{24}\frac{\delta W^{(\mathrm{int})}}{\delta G_{34}}, \qquad (4.25)$$

so that we have for $p>0$

$$\mathbf{G}_{12}^{(p)}=2\int_{34}G_{13}G_{24}\frac{\delta W^{(p)}}{\delta G_{34}} \qquad (4.26)$$

at our disposal to compute the coefficients $\mathbf{G}_{12}^{(p)}$ from removing one line in the connected vacuum diagrams $W^{(p)}$ in all possible ways. The corresponding matrix operations are identical to the ones for cutting a line so that in this respect there is no difference between both procedures to obtain $\mathbf{G}_{12}$.

Combining (4.25) with (2.12), (2.23), and (2.56), we get for the connected four-point function

$$\mathbf{G}^c_{1234}=4\int_{5678}G_{15}G_{26}G_{37}G_{48}\frac{\delta^2 W^{(\mathrm{int})}}{\delta G_{56}\delta G_{78}}$$

$$-4\int_{5678}G_{15}G_{27}(G_{36}G_{48}+G_{46}G_{38})\frac{\delta W^{(\mathrm{int})}}{\delta G_{56}}\frac{\delta W^{(\mathrm{int})}}{\delta G_{78}}, \qquad (4.27)$$

which is equivalent to

$$\mathbf{G}^{c,(p)}_{1234}=4\int_{5678}G_{15}G_{26}G_{37}G_{48}\frac{\delta^2 W^{(p)}}{\delta G_{56}\delta G_{78}}$$

$$-4\sum_{q=1}^{p-1}\binom{p}{q}\int_{5678}G_{15}G_{27}(G_{36}G_{48}+G_{46}G_{38})$$

$$\times\frac{\delta W^{(q)}}{\delta G_{56}}\frac{\delta W^{(p-q)}}{\delta G_{78}}. \qquad (4.28)$$

Again, the sum serves only to subtract disconnected diagrams that are created by the first term, so we may choose to omit the second term and to discard the disconnected diagrams in the first term.

Now the problem of generating diagrams is reduced to the generation of vacuum diagrams and subsequently taking functional derivatives with respect to G_{12}. An advantage of this approach is that external lines do not appear at intermediate steps. So when one uses the cancellation of disconnected terms as a cross check, there are less operations to be performed than with cutting. At the end one just interprets external labels as sitting on external lines. Since all necessary operations on matrices have already been introduced, we

omit examples here and just note that we can again omit external labels if we are not distinguishing between trivially "crossed" diagrams.

The generation of diagrams of the connected two- and four-point functions has been implemented in both possible ways. Cutting or removing one or two lines in the connected vacuum diagrams up to the order $p=6$ leads to the following numbers $n_p^{(2)}$ and $n_p^{(4)}$ of topologically different diagrams of $\mathbf{G}_{12}^{(p)}$ and $\mathbf{G}^{c,(p)}_{1234}$:

p	1	2	3	4	5	6
$n_p^{(2)}$	1	3	8	30	118	548
$n_p^{(4)}$	1	2	8	37	181	1010

$$(4.29)$$

V. OUTLOOK

Using the example of ϕ^4 and $\phi^2 A$ theory, we have developed in this work a new method to generate all topologically different Feynman diagrams together with their proper multiplicities without any combinatorial considerations. Solving a graphical recursion relation leads to the connected vacuum diagrams and a subsequent cutting of their lines results in the connected diagrams. Although our automatization in terms of a MATHEMATICA code [19] turned out to be inefficient in comparison with other, already established programs like FEYNARTS [1–3] or QGRAF [4,5], the construction method as such is conceptually attractive as it immediately follows from the functional integral approach to field theory. As detailed in Sec. IV B, we expect that a sophisticated implementation of our program will be as efficient as existing codes.

In separate publications our method is applied to generate the Feynman diagrams of quantum electrodynamics [21] and one-particle irreducible diagrams in the ordered phase of ϕ^4 theory, where the energy functional contains a mixture of cubic and quartic interactions [22,23]. The work [22] also suggests the capability of our new method beyond a mere generation of graphs. For example, a formal proof of the fact that W generates connected graphs and that the effective energy Γ generates one-particle irreducible graphs could be established. Also, a simple all-orders resummation of perturbation theory is presented there. We believe that our method has great potential in formalizing physically interesting resummations without concern over combinatorics of graphs explicitly, a frequent source of errors in the history of resummations.

It is hoped that our method will eventually be combined with efficient numerical algorithms for actually evaluating Feynman diagrams, e.g., for a more accurate determination of universal quantities in critical phenomena.

[1] J. Külbeck, M. Böhm, and A. Denner, Comput. Phys. Commun. **60**, 165 (1991).

[2] T. Hahn, e-print hep-ph/9905354.

[3] http://www-itp.physik.uni-karlsruhe.de/feynarts

[4] P. Nogueira, J. Comput. Phys. **105**, 279 (1993).

[5] ftp://gtae2.ist.utl.pt/pub/qgraf

[6] H. Kleinert, Fortschr. Phys. **30**, 187 (1982).

[7] H. Kleinert, Fortschr. Phys. **30**, 351 (1982).

[8] B. R. Heap, J. Math. Phys. **7**, 1582 (1966).

[9] J. Neu, M.S. thesis (in German), Freie Universitat Berlin, 1990.

[10] H. Kleinert and V. Schulte-Frohlinde, *Critical Properties of ϕ^4 Theories* (World Scientific, Singapore, 2000).

[11] J. F. Nagle, J. Math. Phys. **7**, 1588 (1966).

[12] B. Kastening, Phys. Rev. D **54**, 3965 (1996).

[13] B. Kastening, Phys. Rev. D **57**, 3567 (1998).

[14] S. A. Larin, M. Mönnigmann, M. Strösser, and V. Dohm, Phys. Rev. B **58**, 3394 (1998).

[15] D. J. Amit, *Field Theory, the Renormalization Group and Critical Phenomena* (McGraw-Hill, New York, 1978).

[16] C. Itzykson and J.-B. Zuber, *Quantum Field Theory* (McGraw-Hill, New York, 1985).

[17] J. Zinn-Justin, *Quantum Field Theory and Critical Phenomena*, 3rd ed. (Oxford University, New York, 1996).

[18] H. Kleinert, *Gauge Fields in Condensed Matter, Vol. I, Superflow and Vortex Lines* (World Scientific, Singapore, 1989).

[19] http://www.physik.fu-berlin.de/˜kleinert/294/programs.

[20] H. Kleinert, J. Neu, V. Schulte-Frohlinde, K. G. Chetyrkin, and S. A. Larin, Phys. Lett. B **272**, 39 (1991); **319**, 545(E) (1993).

[21] M. Bachmann, H. Kleinert, and A. Pelster, Phys. Rev. D **61**, 085017 (2000).

[22] B. Kastening, Phys. Rev. E **61**, 3501 (2000).

[23] A. Pelster and H. Kleinert, e-print hep-th/0006153.